II. Detectors

Energy Deposition

1. Charged particles

Bethe-Bloch formula:

$$-\frac{dE}{dx} = \frac{4\pi q_e^4}{m_0}\frac{z^2}{v^2}\cdot NZ\cdot\left[\ln\frac{2m_0v^2}{I} - \ln\left(1-\beta^2\right) - \beta^2\right]$$

- z, v: atomic number and velocity of projectile
- Z atomic number of absorber
- N Number of absorber atoms per unit volume
- m_0 electron mass
- I absorber ionization energy
- β v/c

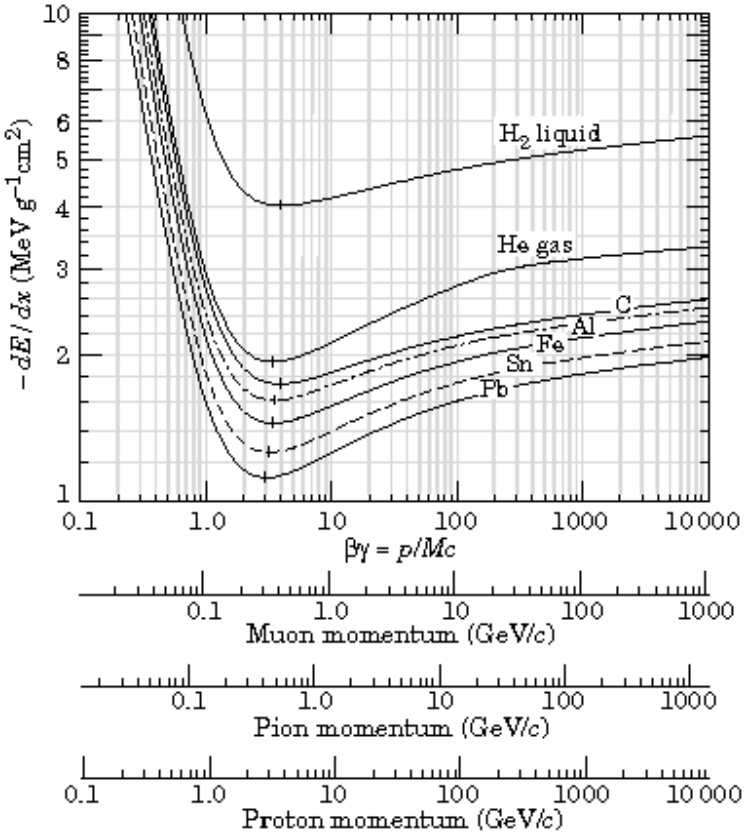

(from *Particle Data Book*)

dE/dx vs. E of protons in silicon

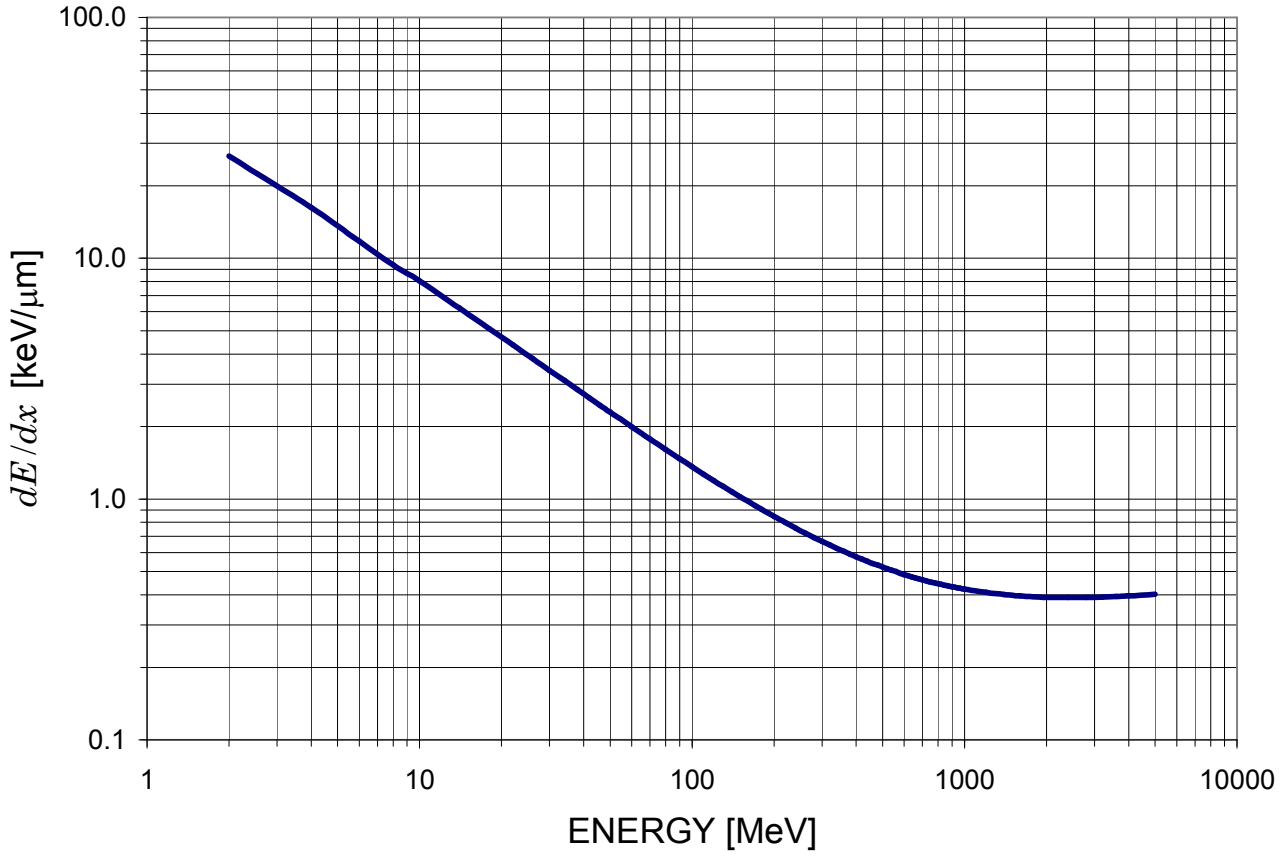

Minimum ionization at 2 – 3 GeV

dE/dx vs. E of electrons in silicon

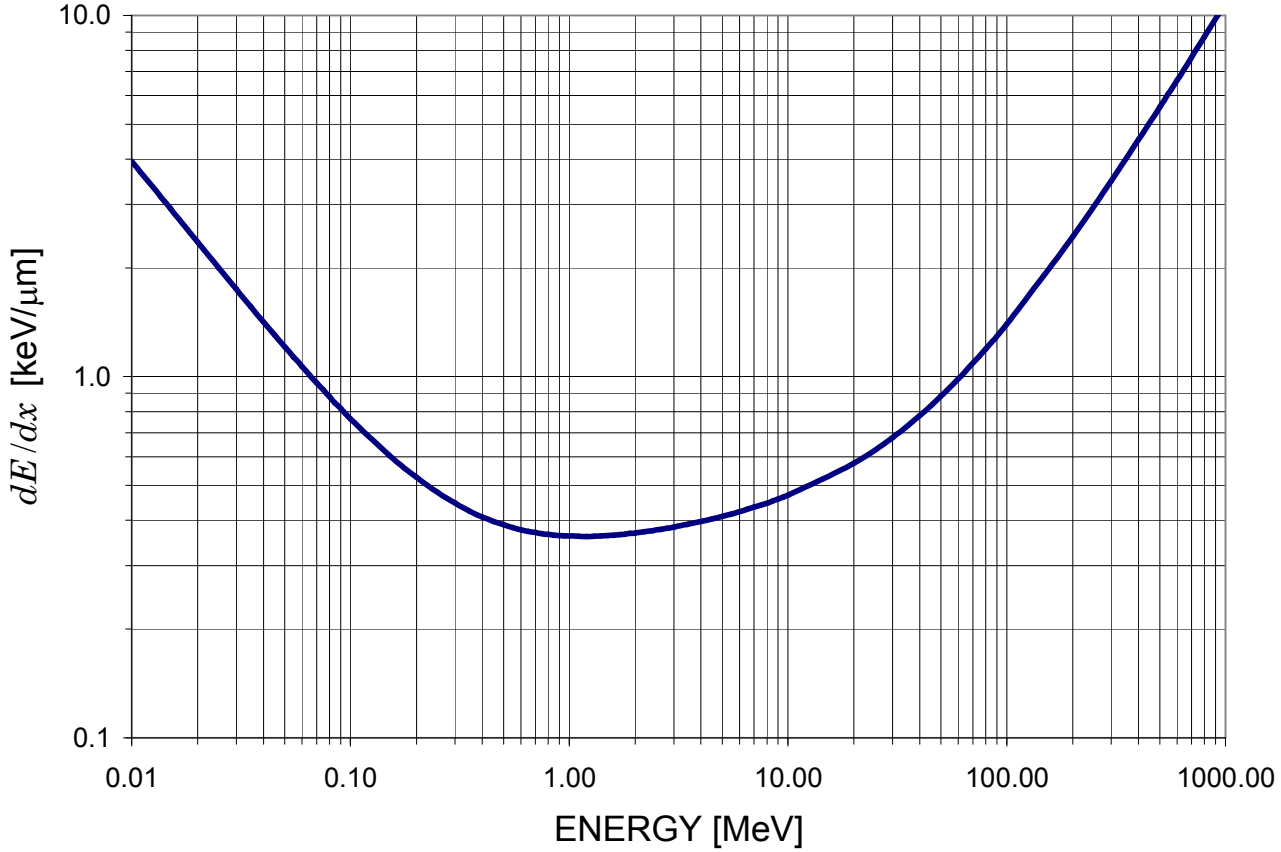

Minimum ionization at ~1 MeV.

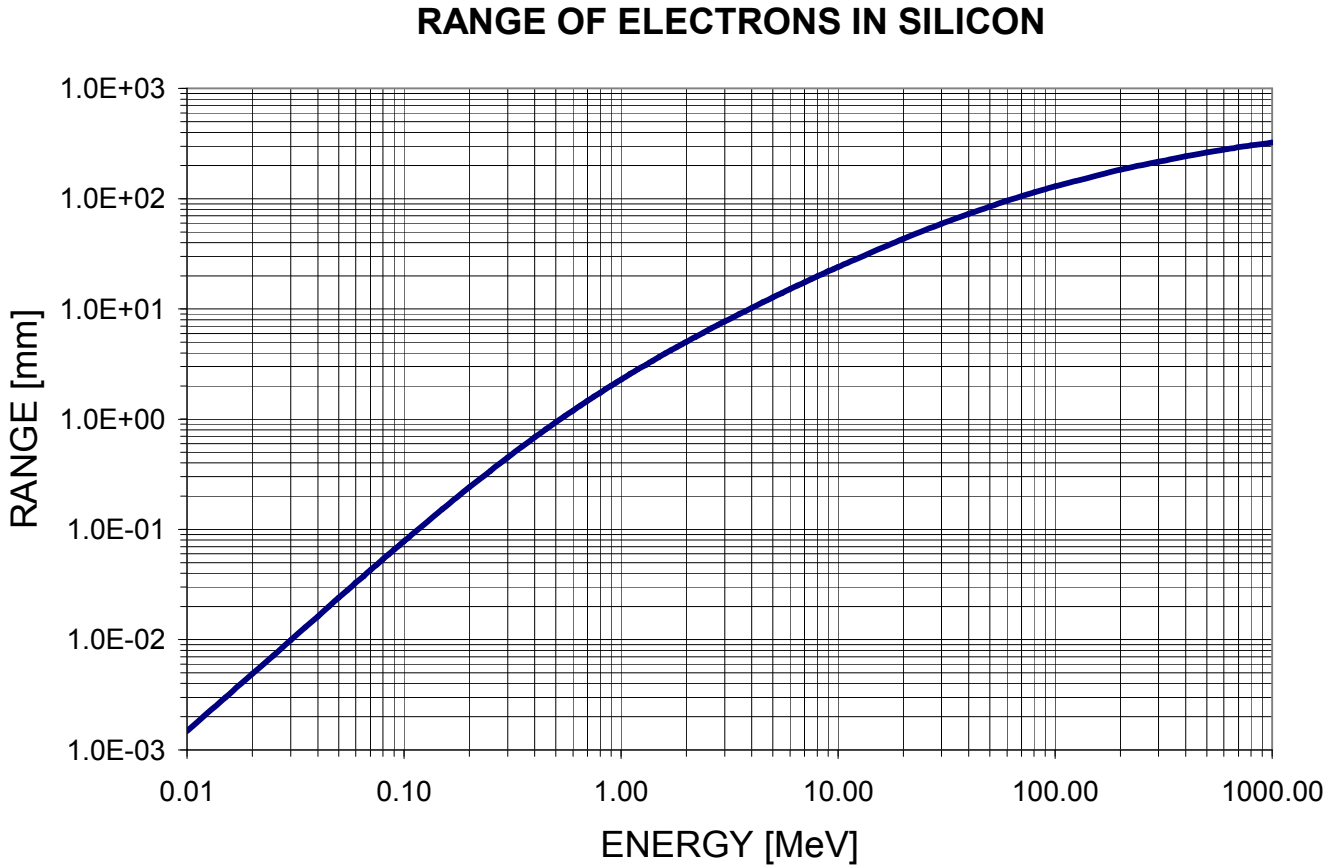

For electrons the range expressed in g cm^{-2} is practically the same in all absorbers.

If the range-energy curve is known for one material, it can be translated to other materials by simple scaling.

$$r_1 \ \rho_1 = r_2 \ \rho_2$$

Energy loss increases for more massive projectiles

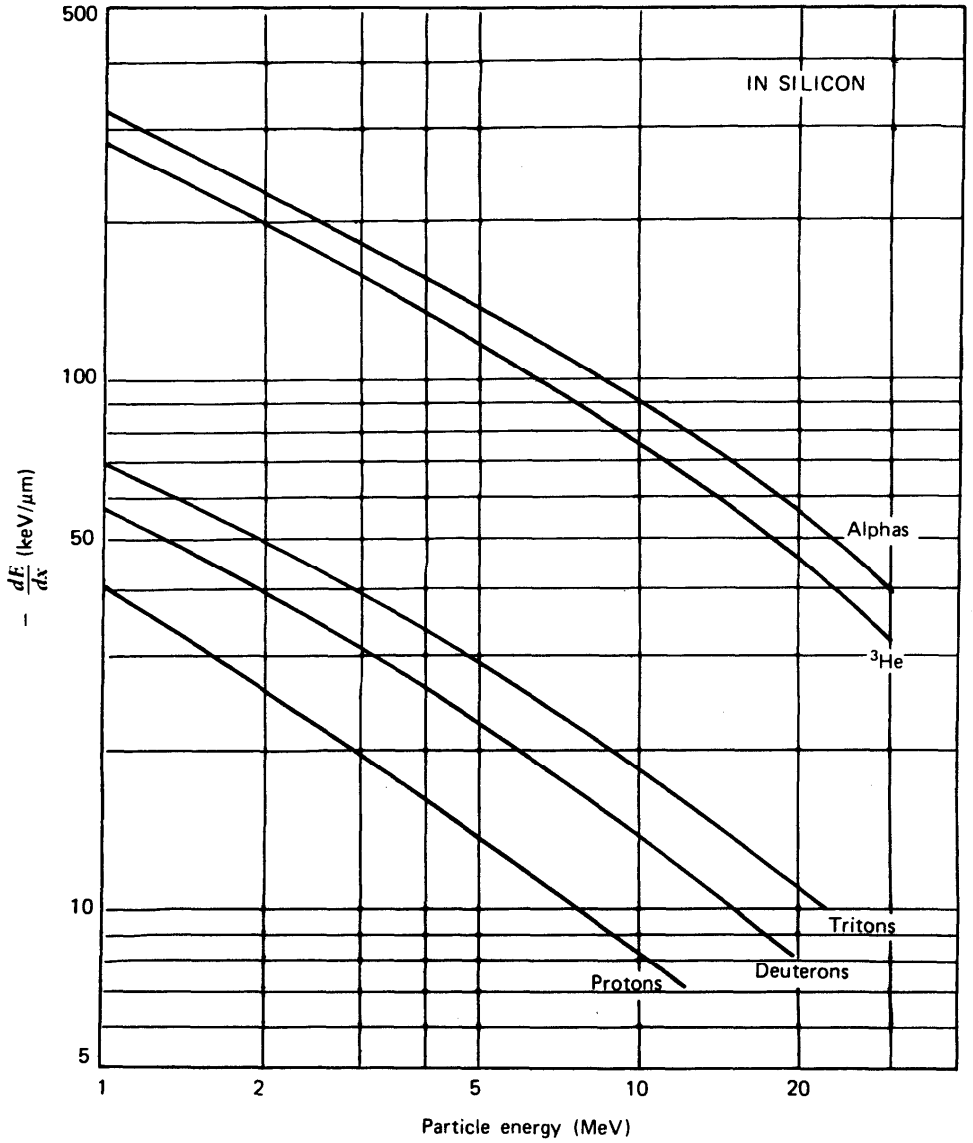

(from Knoll)

At low energies the range of particles decreases drastically with increasing projectile charge.

For E= 5 MeV in Si:

p	R= 220 μm
α	R= 25 μm
^{16}O	R= 4.3 μm
^{40}Ca	R= 3.0 μm
^{132}Xe	R= 2.0 μm
^{197}Au	R= 1.4 μm

2. Neutrons

Cross section much smaller (no Coulomb interaction).

Energy deposition due to knock-on collisions that displace absorber atoms, which deposit energy as charged particles.

Maximum recoil energy transferred to a nucleus of mass number A for head-on collision

$$E_{\max} = \frac{4A}{(A+1)^2} E_n$$

Maximum for protons ($E_{max} = E_n$), whereas for C $E_{max} = 0.35E_n$

Hydrogenous absorber most effective as neutron detectors $\Rightarrow$ plastics

For fast neutrons up to 10 MeV the scattering is isotropic in the center-of-mass system, so the energy distribution of the recoil protons is uniform from $E_p = 0$ to $E_p = E_n$.

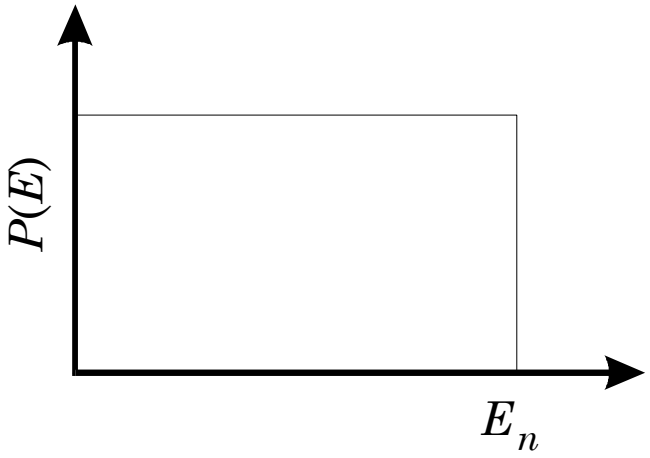

3. Interactions of Gamma Rays

In contrast to charged particles, which deposit energy continuously along their track, photon interactions are localized.

In passing through a medium, photons will traverse a certain distance unaffected, until depositing energy either by

a) photoelectric absorption

b) Compton scattering

c) pair production

The probability of undergoing an interaction is an exponential function of distance. The fraction of photons that suffered any interaction after traversing a distance x is

$$f = 1 - \exp(-\mu\ x)$$

where μ is a linear absorption coefficient, expressed in cm^{-1}, which is the sum of the individual absorption coefficients of the relevant interactions.

The absorption can be parameterized more generally by the mass attenuation coefficient μ / ρ, expressed in $cm^2 g^{-1}$, which is independent of the density or physical state of the absorber.

Gamma Absorption Coefficient in Si vs. Energy

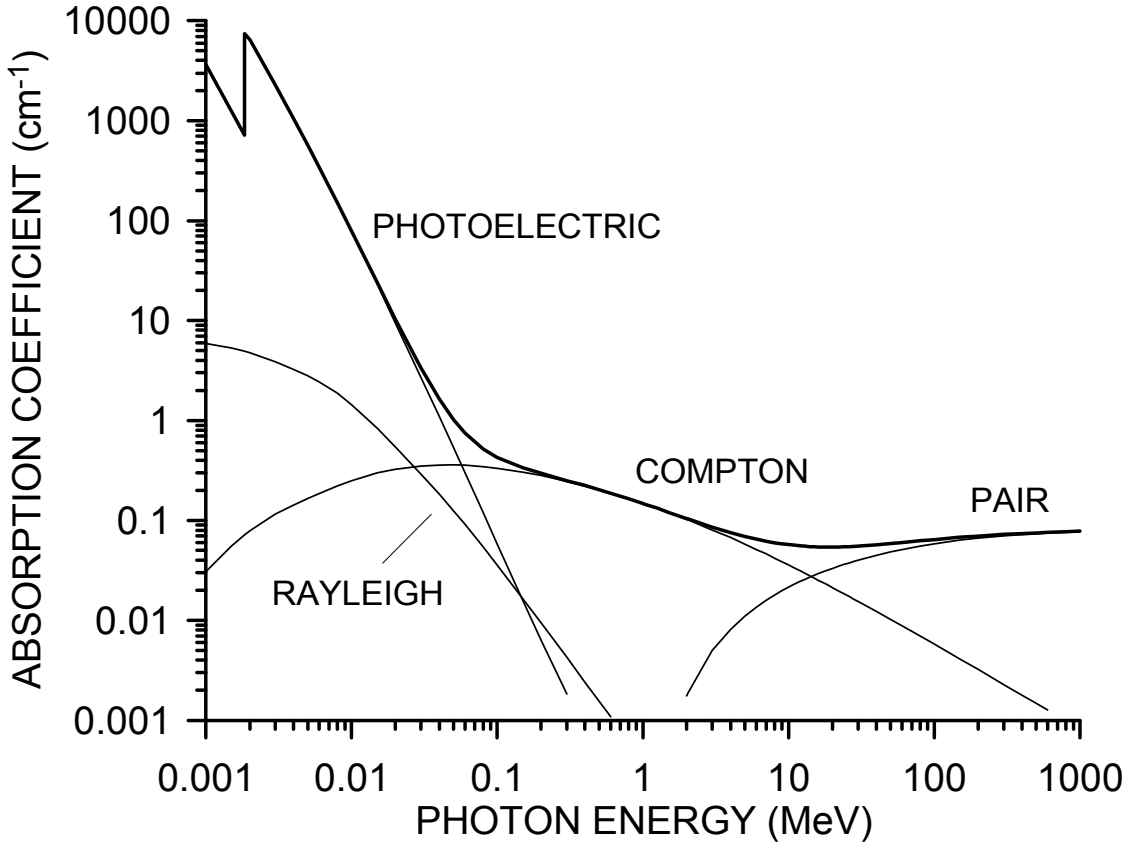

Absorption increases with density and atomic number

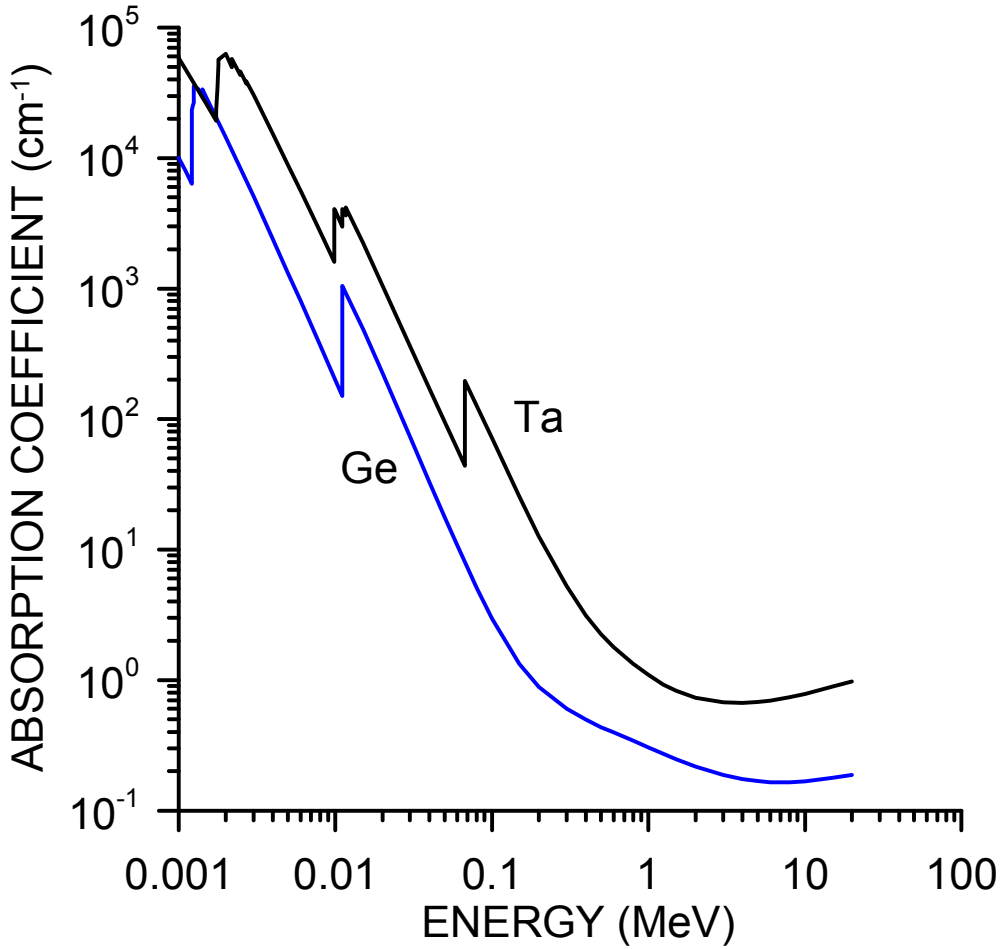

Applies to any phase, e.g. Xe gas

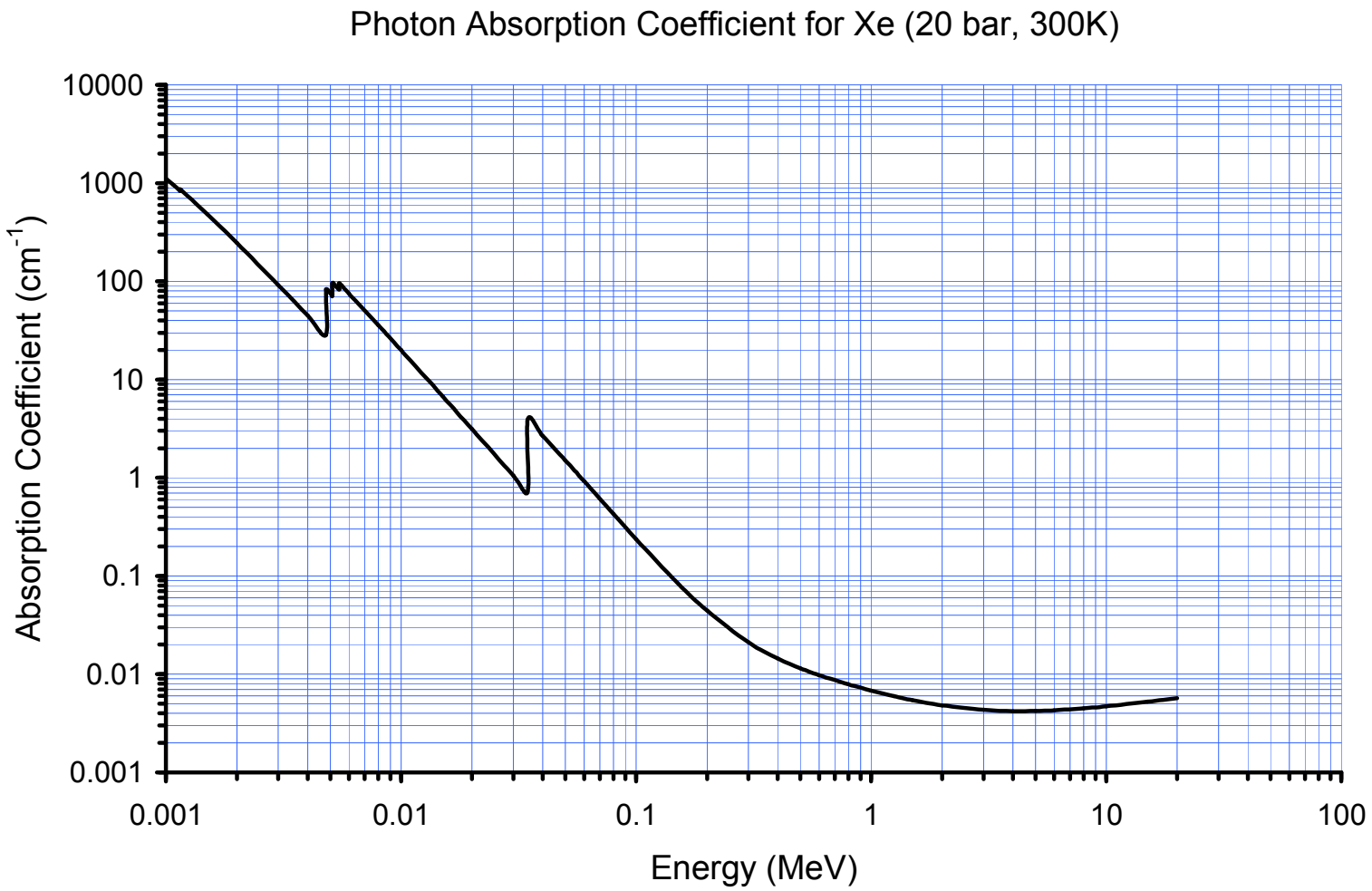

Detector Types

1. Scintillators

Sources:

J.B. Birks, *The Theory and Practice of Scintillation Counting*, New York, 1964
G.F. Knoll, *Radiation Detection and Measurement*, New York, 1989
S.E. Derenzo, *Scintillation Counters, Photodetectors and Radiation Spectroscopy*, IEEE Short Course *Radiation Detection and Measurement*, 2008 IEEE Nuclear Science Symposium

- Incident particles or photons excite atoms or molecules in the scintillating medium.
- Excited states decay under emission of photons, which are detected and converted into electric signals.

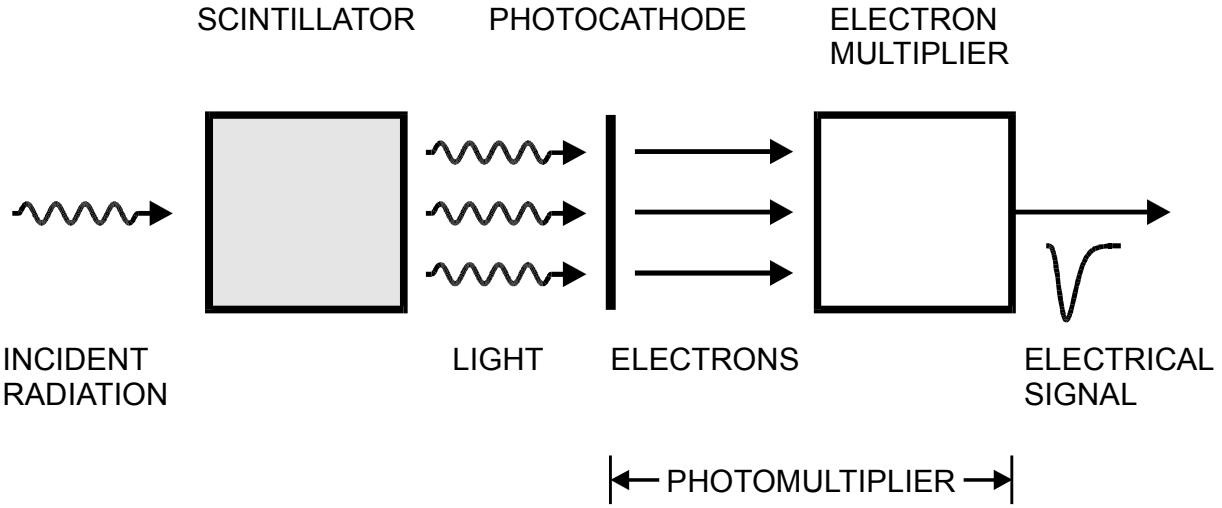

Scintillation materials

Both organic and inorganic materials, can be solid, liquid or gaseous

1. Organic scintillators (e.g. plastics)

a) At room temperature practically all electrons in ground state.
(since S_1 states $\gg 0.025$ eV)

b) Incident radiation populates S_1 states

Vibrational levels within S_1 band decay radiation-less to S_1 base state, which in turn decays under emission of light to the S_0 band.

c) S_1 can also decay to adjacent triplet levels.
Since their energy is significantly lower, the decay time is much longer.

Typical energy levels
(from Birks, as redrawn by Derenzo)

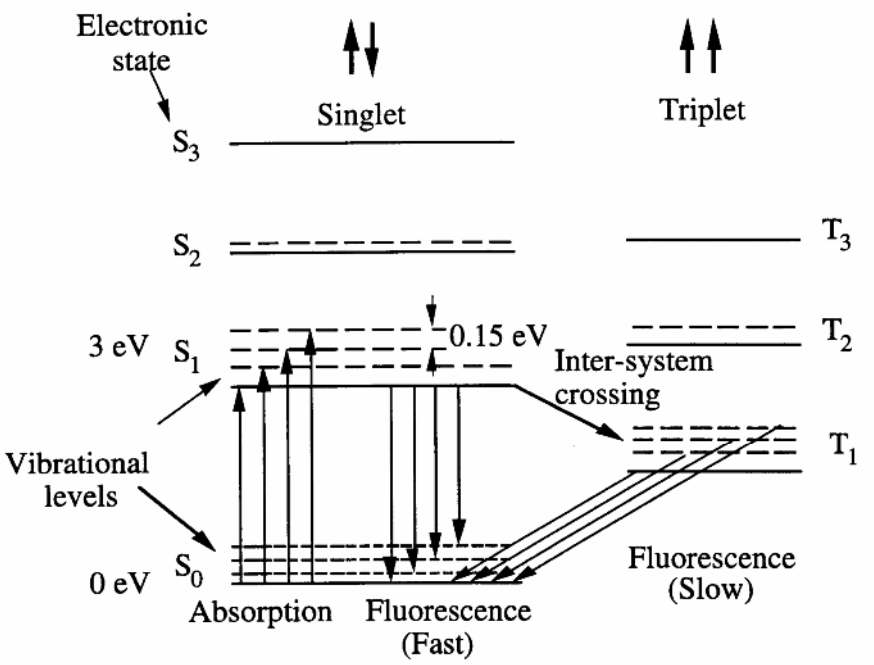

Why isn't emitted light re-absorbed?

If emission and absorption occur at the same wavelengths, most emitted photons would be absorbed within a short distance,

⇒ poor light output from large volume scintillators

Since excitation goes to higher vibrational states in the S_1 band, whereas decay goes from the base S_1 state, the emission spectrum is shifted to lower energies (longer wavelengths).

⇒ only small overlap of emission and absorption spectra

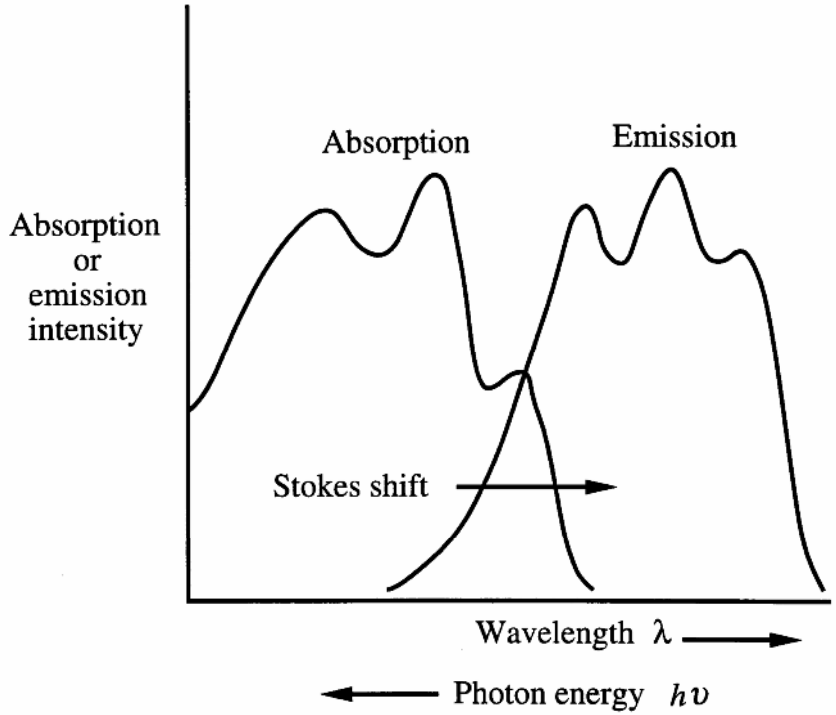

Time dependence of emitted light

a) non-radiative transfer of energy from vibrational states to fluorescent state

typical time: 0.2 – 0.4 ns

b) decay of fluorescent state

typical time: 1 – 3 ns

$\Rightarrow$ rise with time constant τ_r: $I(t) \propto 1 - e^{-t/\tau_r}$

fall with time constant τ_f: $I(t) \propto e^{-t/\tau_f}$

total pulse shape: $I(t) \approx I_0(e^{-t/\tau_f} - e^{-t/\tau_r})$

Rise time usually increased substantially by subsequent components in system and variations of path length in large scintillators.

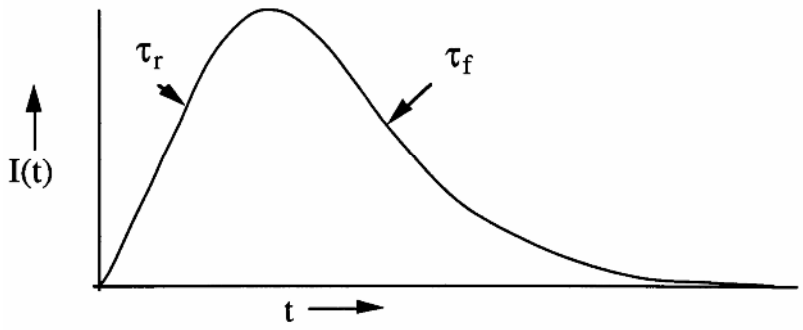

Properties of some typical organic scintillators

Material	State	λ_{max} [nm]	τ_f [ns]	ρ [g/cm^3]	photons/MeV
Anthracene	crystal	447	30	1.25	$1.6 \cdot 10^4$
Pilot U	plastic	391	1.4	1.03	$1.0 \cdot 10^4$
NE104	plastic	406	1.8	1.03	$1.0 \cdot 10^4$
NE102	liquid	425	2.6	1.51	$1.2 \cdot 10^4$

Pilot U, NE104 and NE102 are manufacturers' designations

Inorganic Scintillators

Band structure in inorganic crystals

If forbidden band $\gg kT$,
no electrons in conduction band.

$\Rightarrow$ Insulator

Radiation excites electrons from valence into conduction band, forming electron-hole pairs.

Electrons in the conduction band and holes in the valence band can move freely throughout crystal.

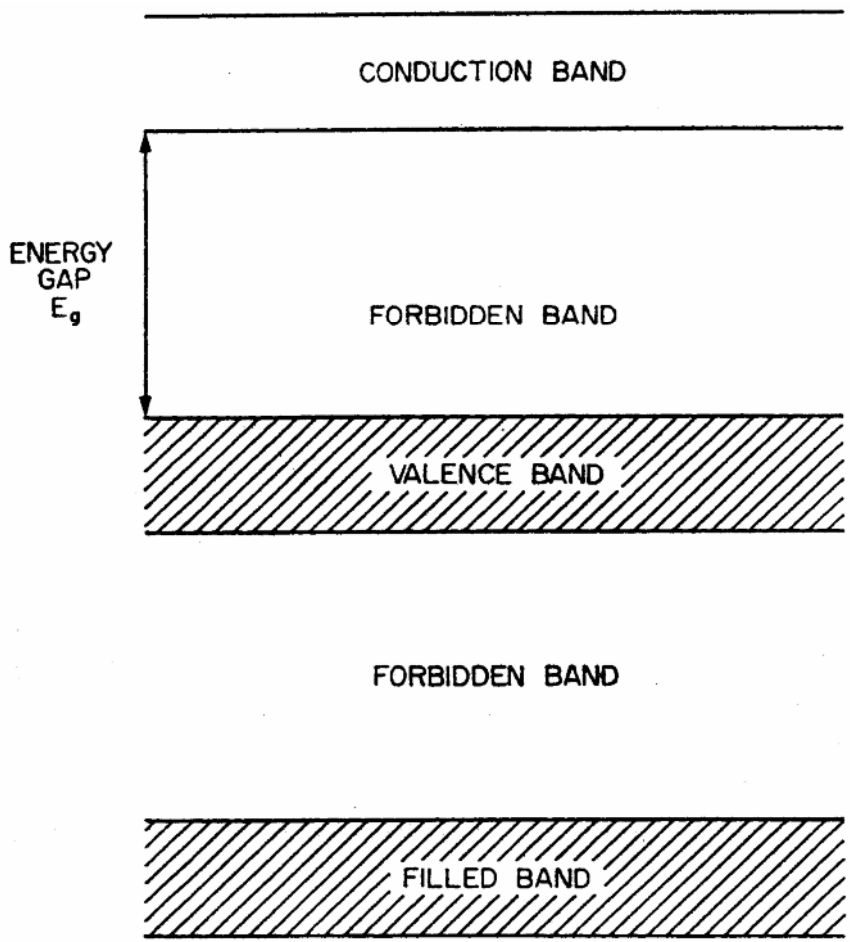

For light emission, one must introduce states into the forbidden band, so that

$$E_{emission} < E_g$$

Light is emitted when these states decay.

Three mechanisms:

a) excitons (bound electron-hole pair)

b) defects (interstitial atoms, for example induced by heat treatment)

c) activators: very dilute concentrations of specific atoms can greatly increase light output

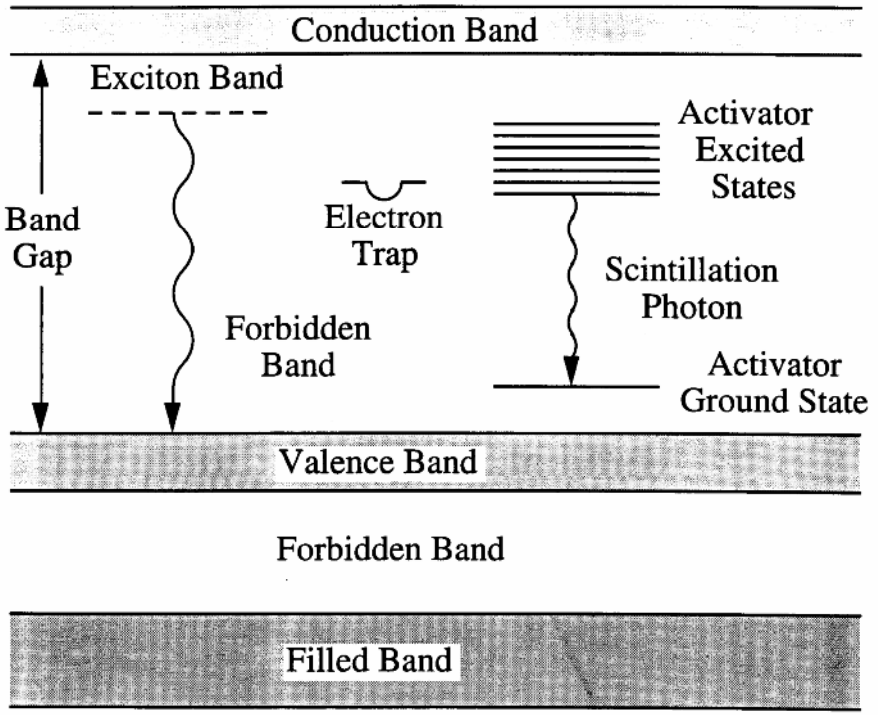

(from Derenzo)

Summary of practical inorganic scintillator materials
(from Derenzo)

Material	Form	λ_{max} (nm)	τ_f (ns)	ρ (g/cm^3)	Photons per MeV
NaI(Tl) (20°C)	crystal	415	230	3.67	38,000
pure NaI (-196°C)	crystal	303	60	3.67	76,000
$Bi_4Ge_3O_{12}$ (20°C)	crystal	480	300	7.13	8,200
$Bi_4Ge_3O_{12}$ (-100°C)	crystal	480	2000	7.13	24,000
CsI(Na)	crystal	420	630	4.51	39,000
CsI(Tl)	crystal	540	800	4.51	60,000
CsI (pure)	crystal	315	16	4.51	2,300
CsF	crystal	390	2	4.64	2,500
BaF_2 (slow)	crystal	310	630	4.9	10,000
BaF_2 (fast)	crystal	220	0.8	4.9	1,800
Gd_2SiO_5(Ce)	crystal	440	60	6.71	10,000
$CdWO_4$	crystal	530	15000	7.9	7,000
$CaWO_4$	crystal	430	6000	6.1	6,000
CeF_3	crystal	340	27	6.16	4,400
$PbWO_4$	crystal	460	2, 10, 38	8.2	500

Note the wide range of decay times τ_f, from 0.8 ns in BaF_2 to 15 μs in $CdWO_4$.
Some materials also show multiple emissions (BaF_2, $PbWO_4$).

Light detection by photomultipliers or semiconductor photodiodes

Photomultipliers most common.

Gain without introducing noise.

Quantum efficiency 10 – 30%

(ratio of electrons emitted photocathode to incident scintillation photons)

Si photodiodes have high quantum efficiency (~90%), but sensitivity is limited by electronic noise.

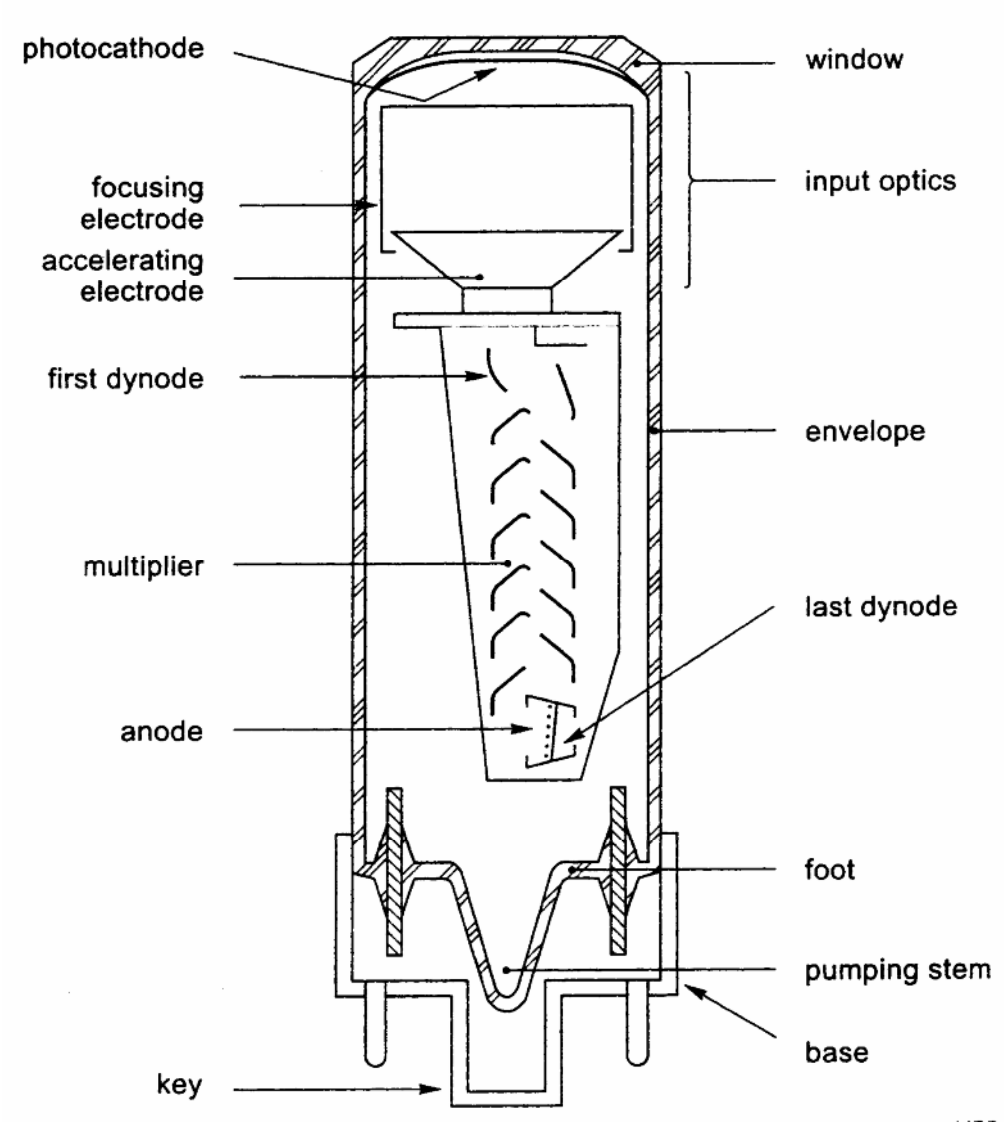

from

2. Semiconductor Detectors

Sensitive volume formed by reverse biasing a semiconductor diode

Incident radiation creates electron-hole pairs (3.6 eV per pair in Si, 2.9 eV in Ge)

Electrons and holes move under applied field $\Rightarrow$ signal current

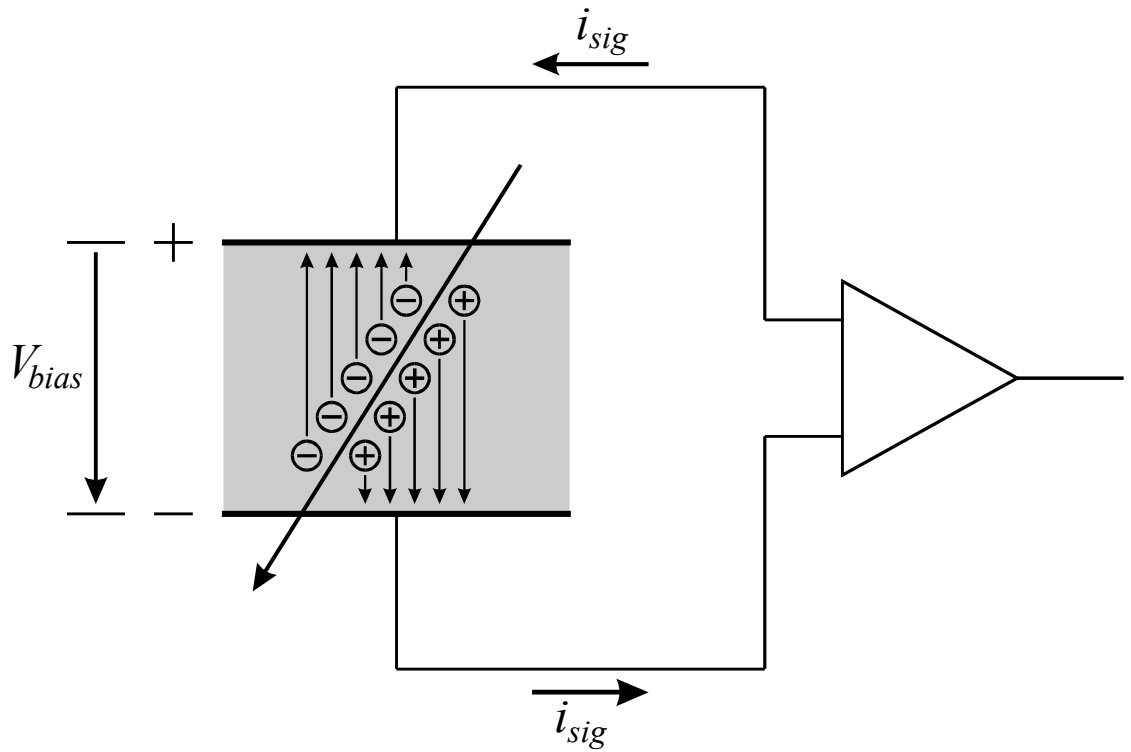

Electrode configurations can be segmented to provide position sensing.

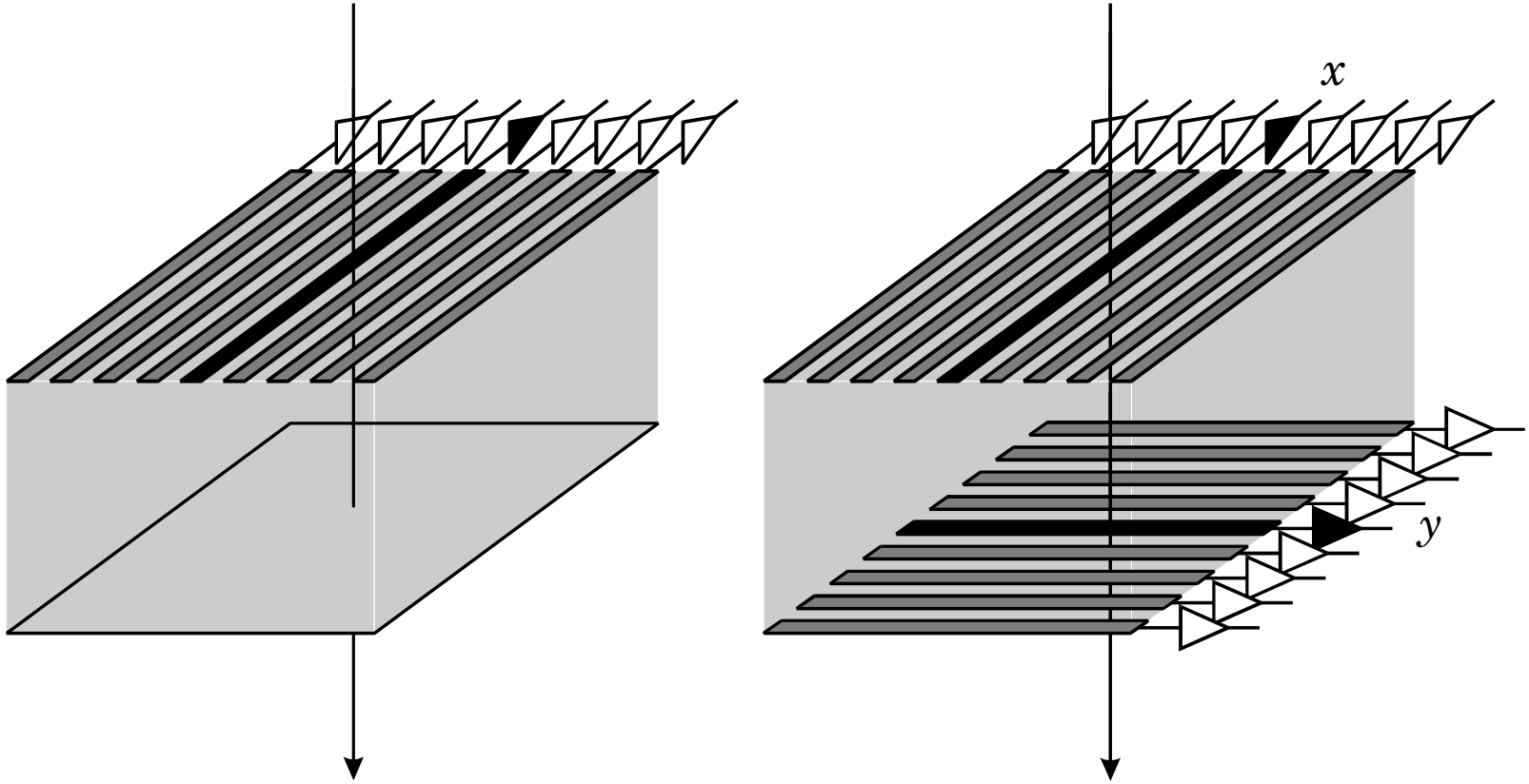

Detector diodes are usually asymmetrically doped. The starting material (bulk) is lightly doped and the junction is formed by diffusing or ion-implanting a highly doped layer.

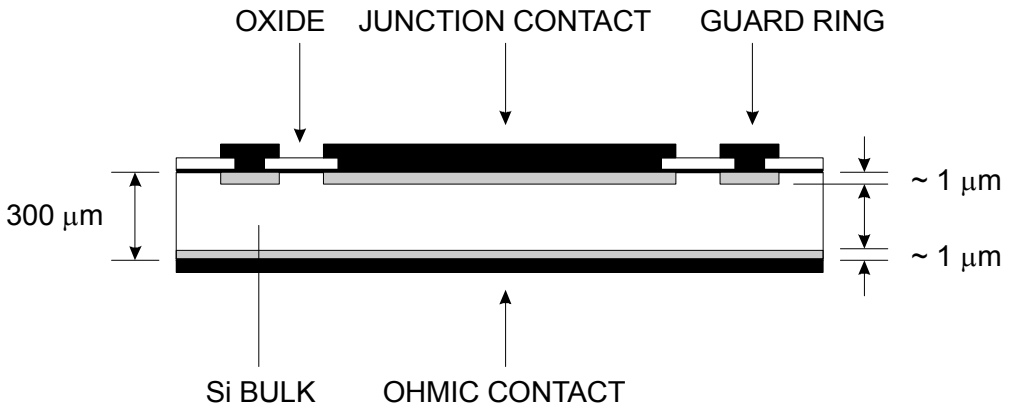

The external connection to the lightly doped bulk is made by an additional highly doped layer of the same type (non-rectifying, “ohmic” contact).

- The depletion region then extends predominantly into the lightly doped bulk.

Other details:

The guard ring isolates the wafer edge (saw cut) from the active region.

In the gap between the detector electrode and the guard ring it is critical to provide a neutral interface at the silicon surface to prevent formation of a conductive path.

This is best accomplished by oxide passivation (SiO_2).

Strip and pixel detectors utilize a similar structure, except that the pn-junction is segmented:

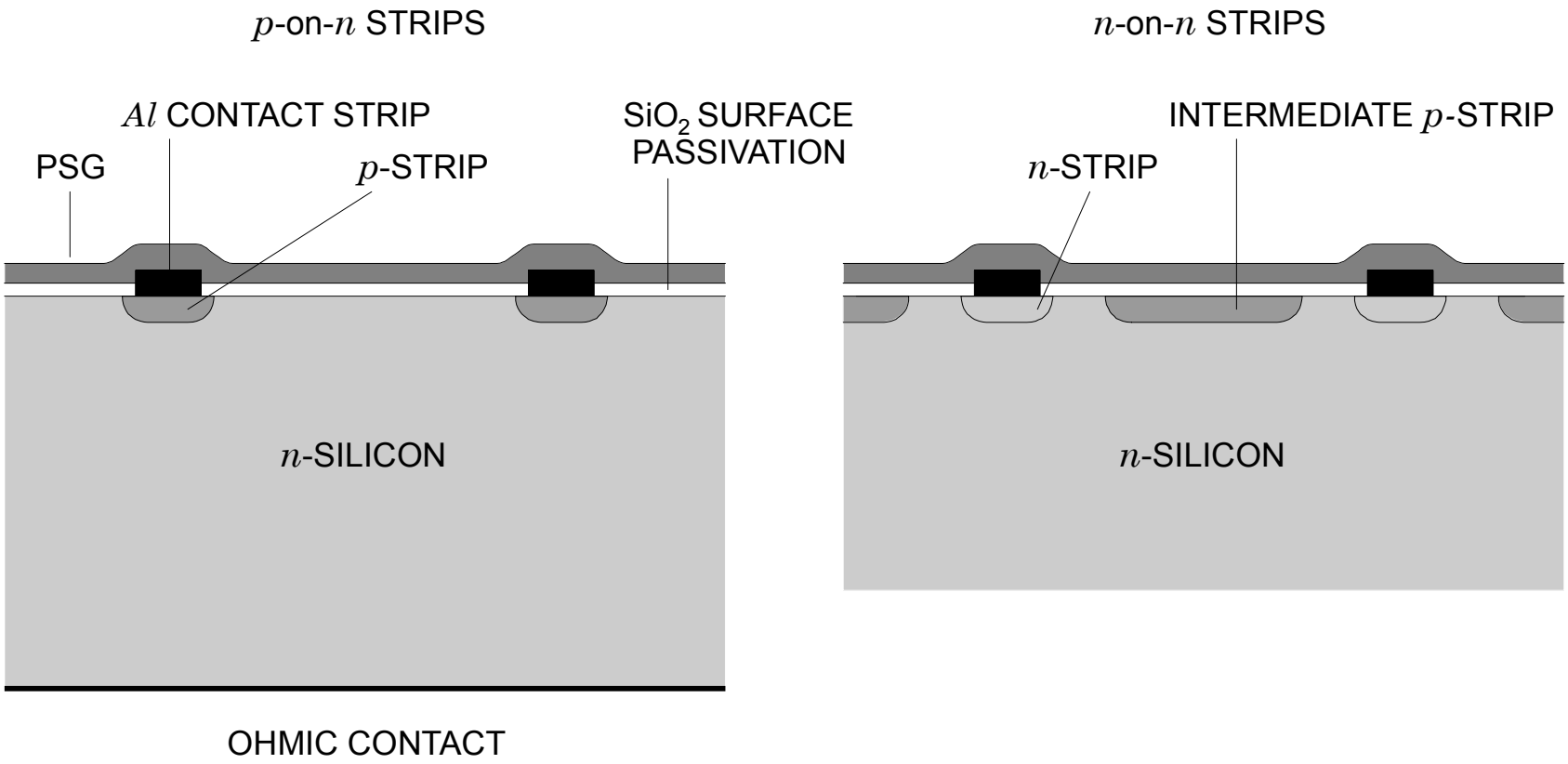

The depletion region extends predominantly into the n-side and the total depletion width is

$$W \approx x_n = \sqrt{\frac{2\varepsilon V_b}{q_e N_d}} \ .$$

The doping concentration is commonly expressed in terms of resistivity

$$\rho = (\mu q_e N)^{-1},$$

because this is a readily measurable quantity. The parameter μ describes the relationship between the applied field and carrier velocity (to be discussed later).

Using resistivity the depletion width becomes

$$W = \sqrt{2\varepsilon \mu_n \rho_n V_b} \ .$$

Note that this introduces an artificial distinction between the n- and p-regions, because the mobilities μ for electrons and holes are different.

Since the mobility of holes is approximately 1/3 that of electrons, p-type material of a given doping concentration will have 3 times the resistivity of n-type material of the same concentration.

Typical resistivities are 1 – 10 kΩ·cm (doping levels ~10^{11} – 10^{12} cm-3)

In transistors and ICs doping levels are typically orders of magnitude higher.

Even in the absence of an external voltage electrons and holes to diffuse across the junction, establishing a "built-in" reverse bias voltage V_{bi}.

If we take this inherent bias voltage into account and set for the bias voltage $V_b \rightarrow V_b + V_{bi}$, one obtains for the one-sided junction

$$W \approx x_1 = \sqrt{\frac{2\varepsilon(V_b + V_{bi})}{q_e N_d}} = \sqrt{2\varepsilon\mu_n\rho_n(V_b + V_{bi})}\ .$$

For example, in n-type silicon (V_b in volts and ρ in Ω·cm):

$$W = \ 0.5\ \mu m\ \mathrm{x}\ \sqrt{\rho(V_b + V_{bi})}$$

and in p-type material:

$$W = \ 0.3\ \mu m\ \mathrm{x}\ \sqrt{\rho(V_b + V_{bi})}\ .$$

Because of the “built-n” voltage diodes can be sensitive to radiation without any applied bias.

The depleted junction volume is free of mobile charge and thus forms a capacitor, bounded by the conducting p- and n-type semiconductor on each side.

The capacitance is

$$C = \varepsilon \frac{A}{W} = A \sqrt{\frac{\varepsilon \; q_e N}{2(V_b + V_{bi})}}$$

For bias voltages $V_b \gg V_{bi}$

$$C \propto \frac{1}{\sqrt{V_b}}$$

In technical units

$$\frac{C}{A} = \frac{\varepsilon}{W} \approx \; 1 \; [\mathrm{pF/cm}] \; \frac{1}{W}$$

A diode with 100 μm thickness has about 1 pF/mm^2.

Charge transport is collision limited, so the velocity of charge carriers depends only on the magnitude of the electric field

$$v = \mu E$$

where the mobility $\mu_e = 1350$ V/cm^{2}s for electrons

$\mu_h = 450$ V/cm^{2}s for holes

This only holds at low fields:

The mobility is constant up to about 10^4 V/cm, but then increased phonon emission reduces the energy going into electron motion, so the mobility decreases. At high fields $E > 10^5$ V/cm the mobility $\mu \propto 1/E$ and carriers attain a constant drift velocity of 10^7 cm/s.

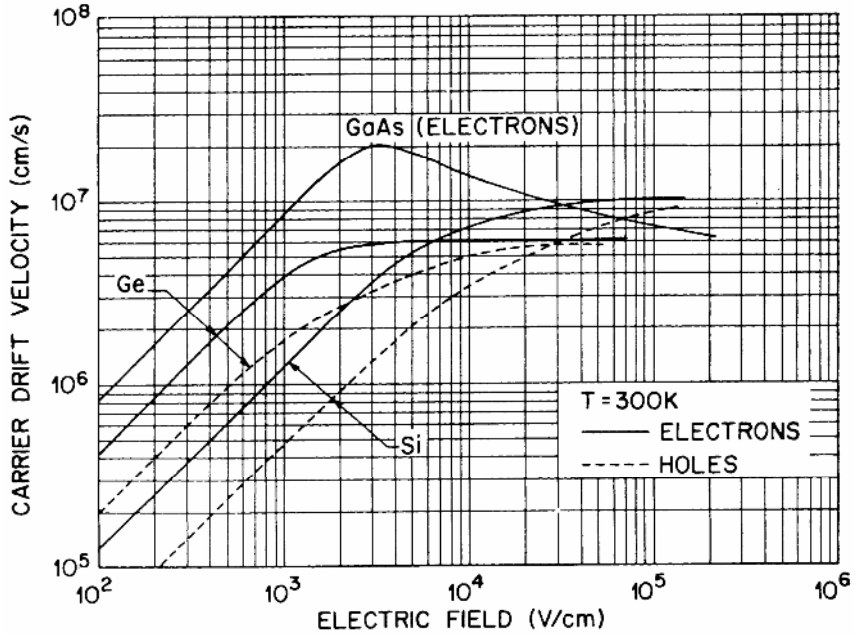

Charge Collection

Mobile electrons and holes formed by radiation move under the influence of the electric field in the junction.

Although electrons and holes move in opposite directions, their contribution to the signal current is of the same polarity.

The time required for a charge carrier to traverse the sensitive volume is called the collection time.

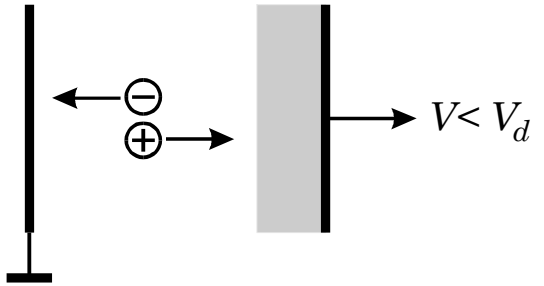

The electric field

$$E(x) = \frac{2(V_b + V_{bi})}{w}\left(1 - \frac{x}{w}\right)$$

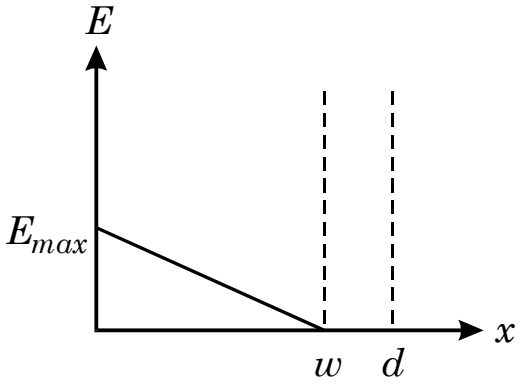

The detector bulk is completely depleted of mobile charge when $W = d$, the thickness of the substrate. This occurs at the externally applied depletion voltage

$$V_d = \frac{q_e N_d W^2}{2\varepsilon} - V_{bi} .$$

Then the field drops linearly from its maximum value at the junction to zero at the opposite contact.

Overbias

Increasing the bias beyond the depletion voltage adds a uniform field due to the voltage beyond depletion, yielding a distribution

$$E(x) = \frac{2V_{di}}{d}\left(1 - \frac{x}{d}\right) + \frac{V_b - V_{di}}{d},$$

where $V_{di} \equiv V_d + V_{bi}$ is the effective depletion voltage.

This signficantly speeds up charge collection, since in partial or full depletion the field goes to zero.

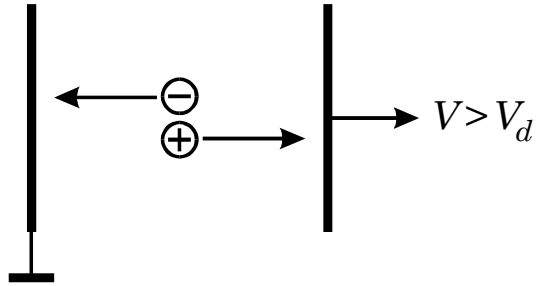

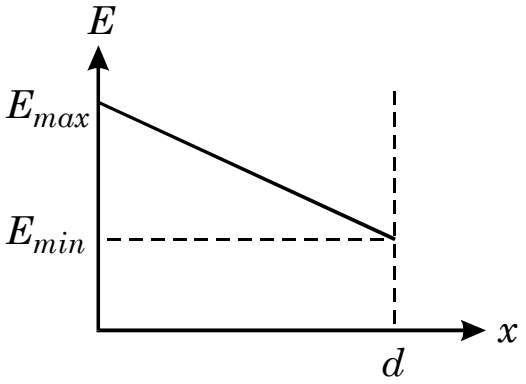

Example:

For n-type silicon of 10 kΩ·cm resistivity,

a detector thickness of 300 μm, and

a reverse bias voltage V_b= 60V= 2V_d (i.e. E_0 =2·10^3 and E_1 =10^3 V/cm)

Collection times for

Electrons: 12 ns

Holes: 36 ns.

This is substantially less than in the partially depleted device, where collection times for

Electrons: 30 ns

Holes: 90 ns.

Time Dependence of the Signal Current

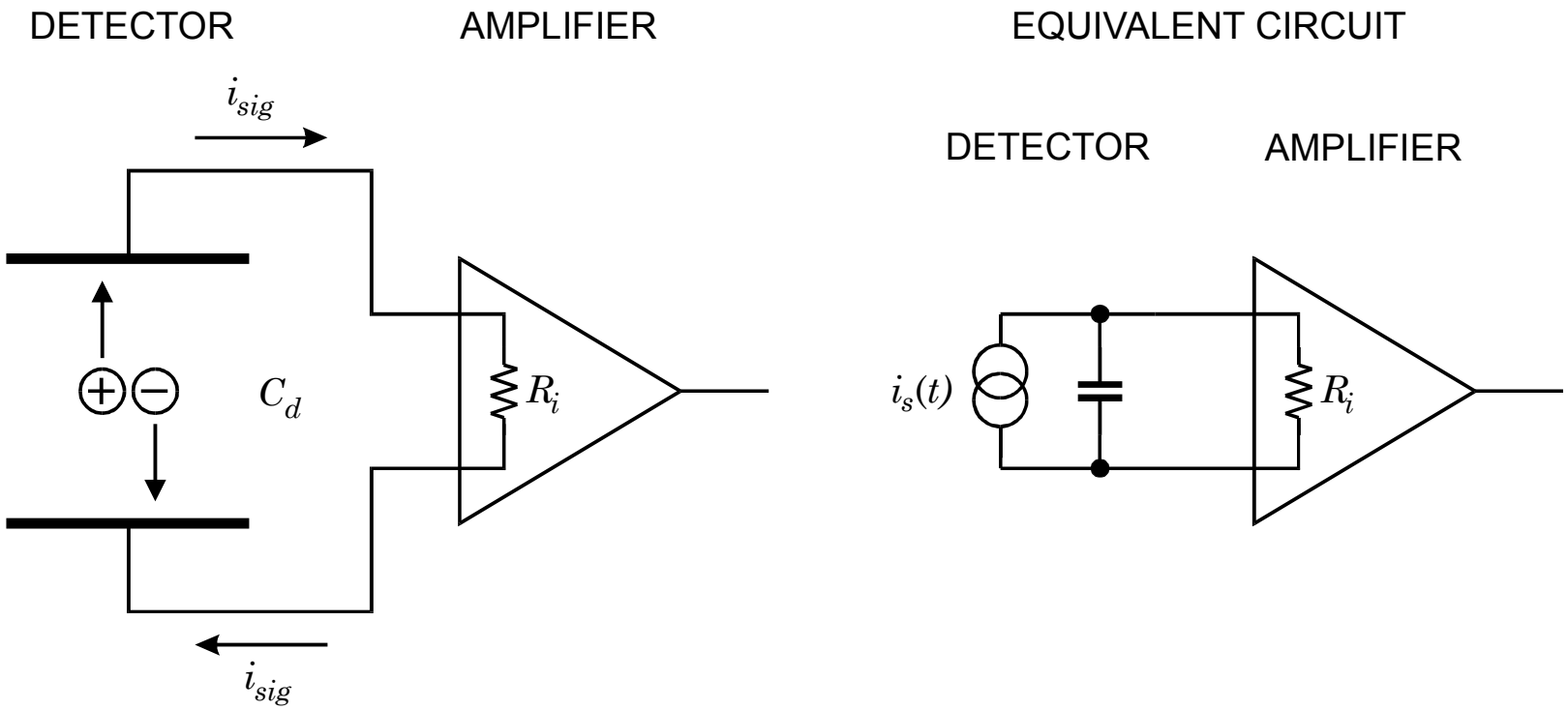

When does the signal current begin?

a) when the charge reaches the electrode?

or

b) when the charge begins to move?

Although the first answer is quite popular (encouraged by the phrase “charge collection”), the second is correct.

When a charge pair is created, both the positive and negative charges couple to the electrodes. As the charges move the induced charge changes, i.e. a current flows in the electrode circuit.

The following discussion applies to ALL types of structures that register the effect of charges moving in an ensemble of electrodes, i.e. not just semiconductor or gas-filled ionization chambers, but also resistors, capacitors, photoconductors, vacuum tubes, etc.

The effect of the amplifier on the signal pulse will be discussed in the Electronics part.

Induced Charge

Consider a charge q in a parallel plate capacitor:

When the charge is midway between the two plates, the charge induced on one plate is determined by applying Gauss' law. The same number of field lines intersect both S_1 and S_2, so equal charge is induced on each plate (= q / 2).

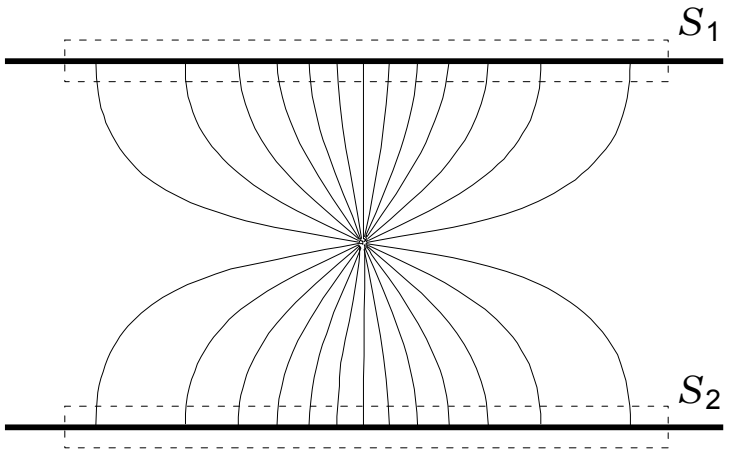

When the charge is close to one plate, most of the field lines terminate on that plate and the induced charge is much greater.

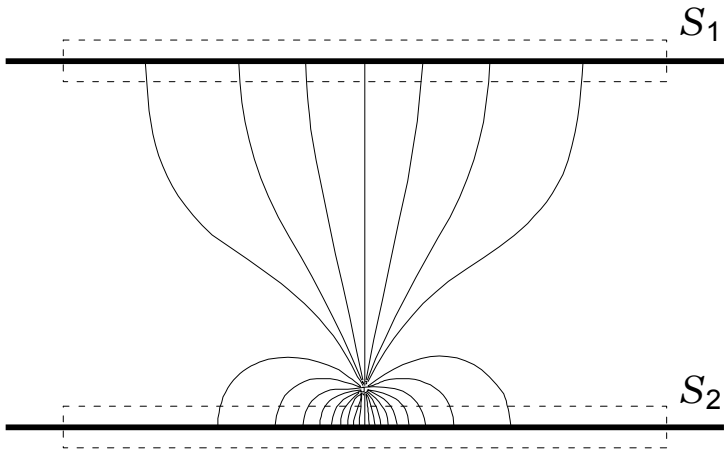

As a charge traverses the space between the two plates the induced charge changes continuously, so current flows in the external circuit as soon as the charges begin to move.

Induced Signal Currents in a Strip Detector

Consider a charge originating near the upper contiguous electrode and drifting down towards the strips.

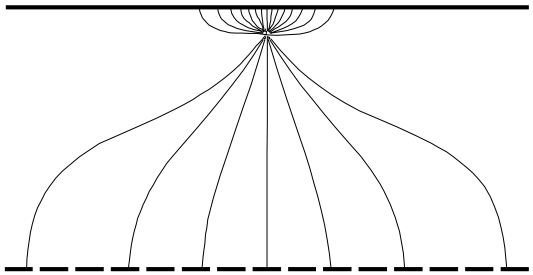

Initially, charge is induced over many strips.

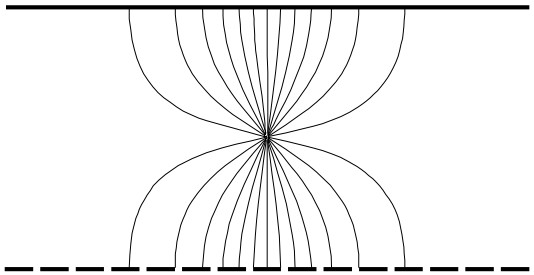

As the charge approaches the strips, the signal distributes over fewer strips.

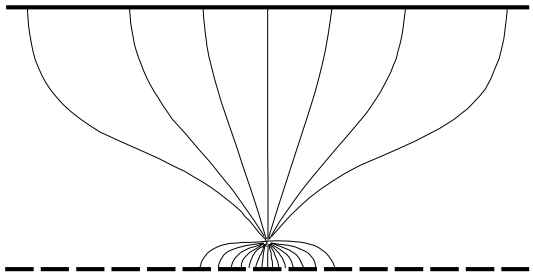

When the charge is close to the strips, the signal is concentrated over few strips

The magnitude of the induced current due to the moving charge depends on the coupling between the charge and the individual electrodes.

Mathematically this can be analyzed conveniently by applying Ramo's theorem.

Induced Charge – Ramo's Theorem

W. Shockley, J. Appl. Phys. **9** (1938) 635
S. Ramo, Proc. IRE **27** (1939) 584

Consider a mobile charge in the presence of any number of grounded electrodes.

Surround the charge q with a small equipotential sphere. Then, if V is the potential of the electrostatic field, in the region between conductors

$$\nabla^2 V = 0$$

Call V_q the potential of the small sphere and note that V= 0 on the conductors. Applying Gauss' law yields

$$\int_{\substack{\text{sphere's}\\ \text{surface}}} \frac{\partial V}{\partial n} ds = 4\pi q$$

Next, consider the charge removed and one conductor A raised to unit potential.

Call the potential V_1, so that

$$\nabla^2 V_1 = 0$$

in the space between the conductors, including the site where the charge was situated. Call the new potential at this point V_{q1}.
Green's theorem states that

$$\int_{\substack{\text{volume between}\\ \text{boundaries}}} (V_1 \nabla^2 V - V\ \nabla^2 V_1)\ dv = \quad - \int_{\substack{\text{boundary}\\ \text{surfaces}}} \left[V_1 \frac{\partial V}{\partial n} - V \frac{\partial V_1}{\partial n} \right] ds\ .$$

Choose the volume to be bounded by the conductors and the tiny sphere.

Then the left hand side is 0 and the right hand side may be divided into three integrals:

1. Over the surfaces of all conductors except A. This integral is 0 since on these surfaces $V = V_1 = 0$.

2. Over the surface of A. As $V_1 = 1$ and $V = 0$ this reduces to

$$- \int_{\text{surface A}} \frac{\partial V}{\partial n} ds\ .$$

3. Over the surface of the sphere.

$$-V_{q1} \int_{\substack{\text{sphere's}\\ \text{surface}}} \frac{\partial V}{\partial n} ds \quad + \quad V_q \int_{\substack{\text{sphere's}\\ \text{surface}}} \frac{\partial V_1}{\partial n} ds\ .$$

The second integral is 0 by Gauss' law, since in this case the charge is removed.

Combining these three integrals yields

$$0 = -\int_{\text{surface A}} \frac{\partial V}{\partial n} ds \quad - \quad V_{q1} \int_{\substack{\text{sphere's} \\ \text{surface}}} \frac{\partial V}{\partial n} ds = 4\pi\ Q_A - 4\pi\ qV_{q1}$$

or $Q_A = qV_{q1}$.

If the charge q moves in direction x, the current on electrode A is

$$i_A = \frac{dQ_A}{dt} = q\frac{dV_{q1}}{dt} = q\left(\frac{\partial V_{q1}}{\partial x}\ \frac{dx}{dt}\right).$$

Since the velocity of motion

$$\frac{dx}{dt} = v_x\ ,$$

the induced current on electrode A is $i_A = q\ v_x \frac{\partial V_{q1}}{dx}$,

where V_{q1} is the “weighting potential” that describes the coupling of a charge at any position to electrode A.

The weighting potential is for a specific electrode is obtained by setting the potential of the electrode to 1 and setting all other electrodes to potential 0.

- If a charge q moves along any path s from position 1 to position 2, the net induced charge on electrode k is

$$\Delta Q_k = q(V_{q1}(2) - V_{q1}(1)) \equiv q\left(\Phi_k(2) - \Phi_k(1)\right)$$

- The instantaneous current can be expressed in terms of a weighting field

$$i_k = -q\ \vec{v} \cdot\ \overrightarrow{F_k}$$

  The weighting field is determined by applying unit potential to the measurement electrode and 0 to all others. For this calculation the electrodes are assumed to be in a vacuum or a uniform dielectric.

- It is not affected by the presence of space charge, as the electric field in a semiconductor detector.

Note that the electric field and the weighting field are distinctly different.

- The electric field determines the charge trajectory and velocity.
- The weighting field depends only on geometry and determines how charge motion couples to a specific electrode. It is field with the unit 1/length (no voltage!) that describes the coupling from the charge at a given position to a specific electrode and has noting to do with work or energy.
- Only in 2-electrode configurations are the electric field and the weighting field of the same form.
- **The detector signal originates as a current!**
  Signal charge is a secondary quantity, obtained by integrating the signal current: $Q_s = \int i_s(t)dt$.

Example 1: Parallel plate geometry with uniform field

(semiconductor detector with very large overbias)

Assume a voltage V_b applied to the detector. The distance between the two parallel electrodes is d.

The electric field that determines the motion of charge in the detector is

$$E = \frac{V_b}{d}$$

Assume that the velocity of the charge carriers is collision limited, so the velocity of the charge

$$v = \mu E = \mu \frac{V_b}{d}$$

The weighting field is obtained by applying unit potential to the collection electrode and grounding the other,

$$E_Q = \frac{1}{d}$$

so the induced current

$$i = qvE_Q = q\mu \frac{V_b}{d}\frac{1}{d} = q\mu \frac{V_b}{d^2}$$

Since both the electric field and the weighting field are uniform throughout the detector, the current is constant until the charge reaches its terminal electrode.

Assume that the charge is created at the opposite electrode and traverses the detector thickness d.

The required collection time, i.e. the time required to traverse the detector thickness d

$$t_c = \frac{d}{v} = \frac{d}{\mu \frac{V_b}{d}} = \frac{d^2}{\mu V_b}$$

The induced charge

$$Q = it_c = q\mu \frac{V_b}{d^2} \frac{d^2}{\mu V_b} = q$$

Next, assume an electron-hole pair formed at coordinate x from the positive electrode.

The collection time for the electron

$$t_{ce} = \frac{x}{v_e} = \frac{xd}{\mu_e V_b}$$

and the collection time for the hole

$$t_{ch} = \frac{d-x}{v_h} = \frac{(d-x)d}{\mu_h V_b}$$

Since electrons and holes move in opposite directions, they induce current of the same sign at a given electrode, despite their opposite charge.

The induced charge due to the motion of the electron

$$Q_e = q_e \mu_e \frac{V_b}{d^2} \frac{xd}{\mu_e V_b} = q_e \frac{x}{d}$$

whereas the hole contributes

$$Q_h = q_e \mu_h \frac{V_b}{d^2} \frac{(d-x)d}{\mu_h V_b} = q_e \left(1 - \frac{x}{d}\right)$$

Assume that $x = d/2$. After the collection time for the electron

$$t_{ce} = \frac{d^2}{2\mu_e V_b}$$

it has induced a charge $q_e/2$.

At this time the hole, due to its lower mobility $\mu_h \approx \mu_e/3$, has induced $q_e/6$, yielding a cumulative induced charge of $2q_e/3$.

After the additional time for the hole collection, the remaining charge $q_e/3$ is induced, yielding the total charge q_e.

In this configuration

- Electrons and holes contribute equally to the currents on both electrodes
- The instantaneous current at any time is the same (although of opposite sign) on both electrodes

The continuity equation (Kirchhoff's law) must be satisfied:

$$\sum_k i_k = 0$$

Since k=2: $i_1 = -i_2$

A Common Fallacy

A widespread derivation of induced charge is based on energy balance, where it is postulated that the energy gained by the particle in traversing the sensor equals the change in potential on the capacitor plates.

This predicts the incremental charge $$dQ = q\frac{dV}{V}$$

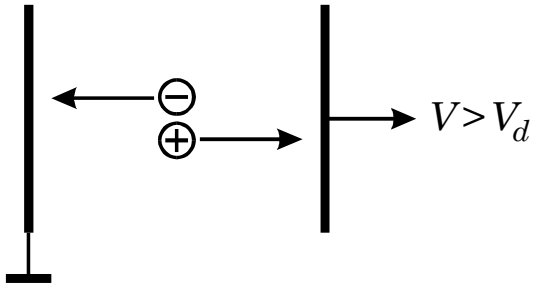

Because the field in a semiconductor detector isn't constant, the potential has a quadratic term, which yields a different pulse shape than derived from electrostatics,

$$dQ = q\frac{dx}{d}.$$

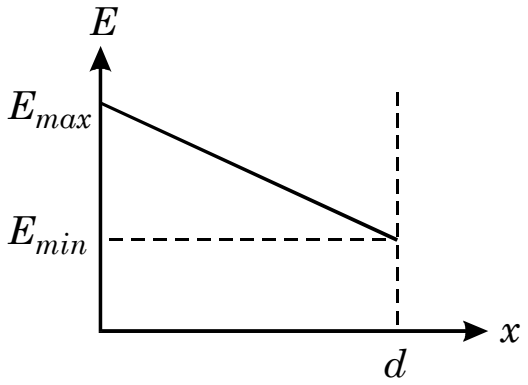

The fundamental error in the energy balance concept is that it assumes that all energy imparted by the field goes into carrier motion, i.e. ballistic transport.

However, most of the energy goes into other modes (phonons). The energy balance approach is false for all collision-limited transport, i.e. in solids, liquids, and gases.

- The induced charge described by Ramo's theorem applies the correct physics for all materials and electrode configurations.

Example 2: Double-Sided Strip Detector

The strip pitch is assumed to be small compared to the thickness.

The electric field is similar to a parallel-plate geometry, except in the immediate vicinity of the strips.

The signal weighting potential, however is very different.

Weighting potential for a 300 μm thick strip detector with strips on a pitch of 50 μm. Only 50 μm of depth are shown.

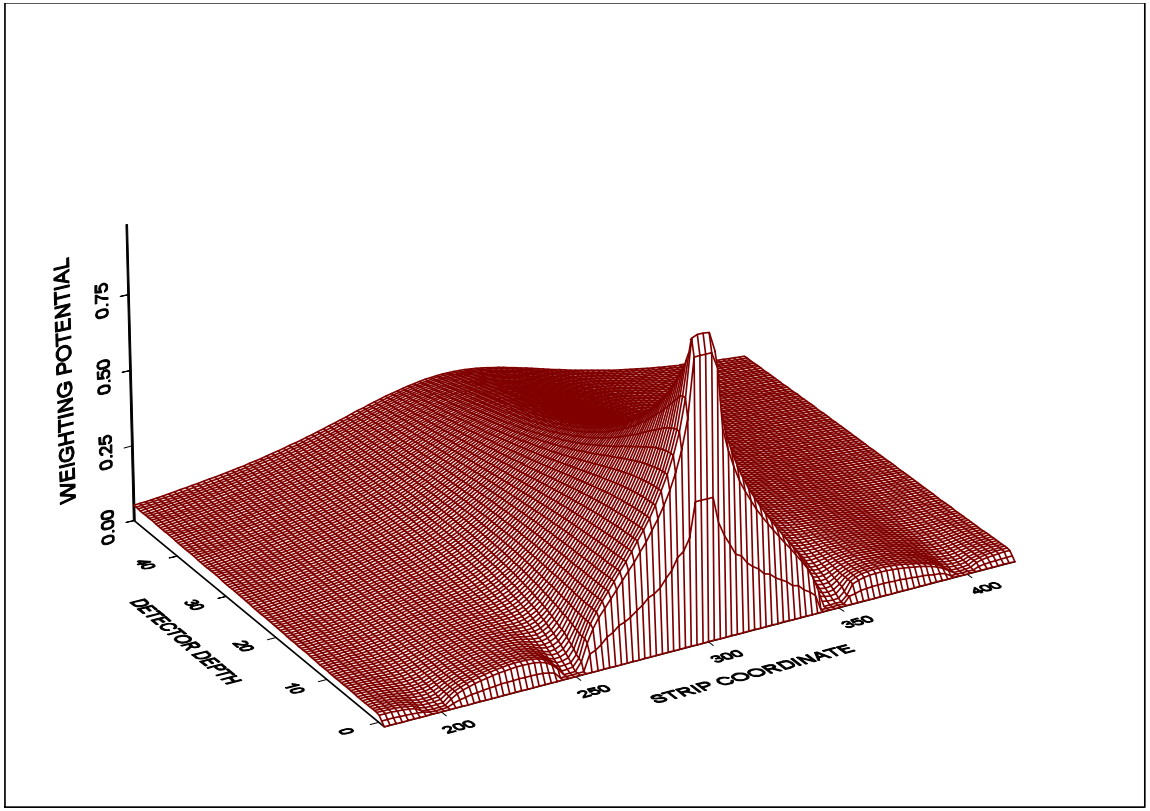

Cuts through the weighting potential

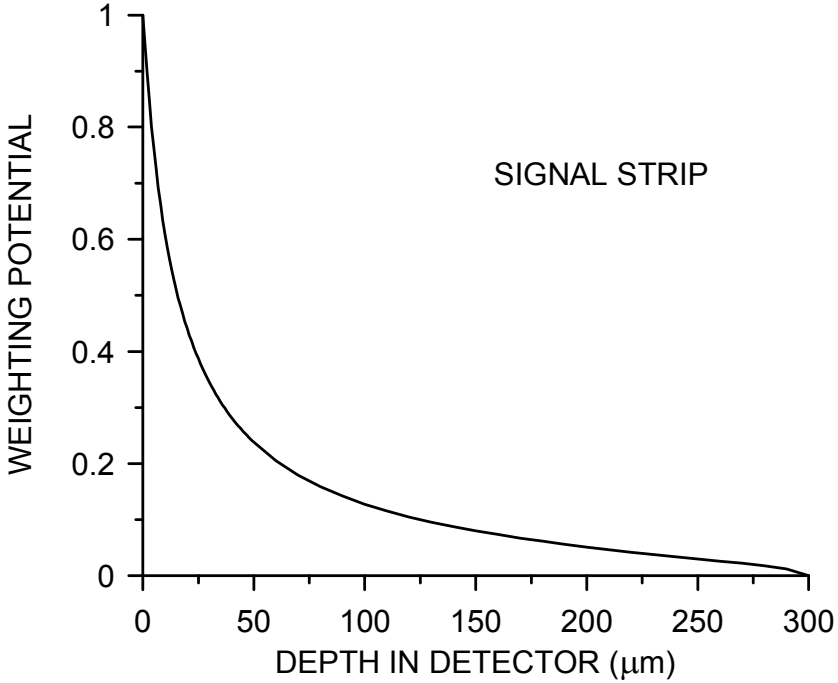

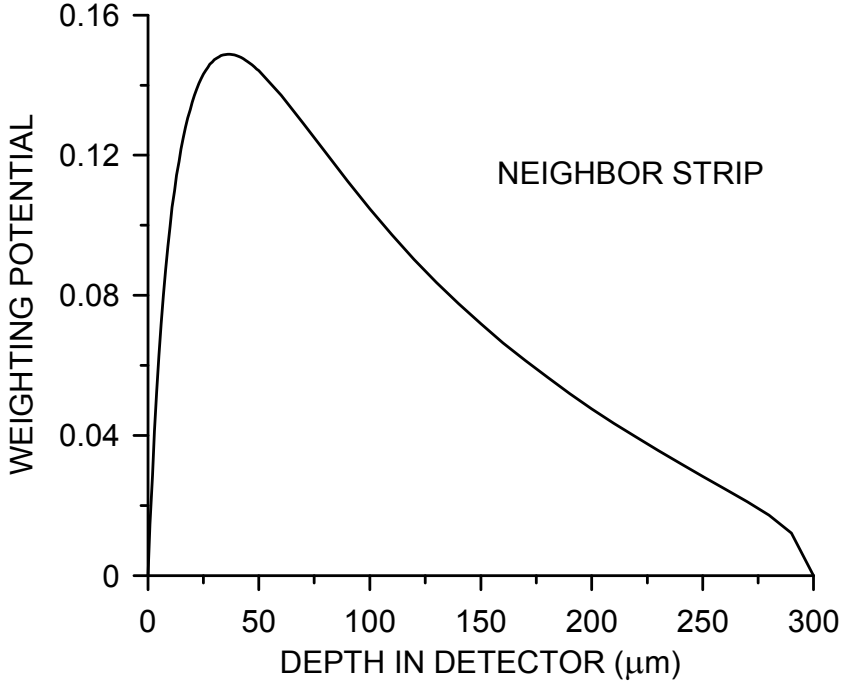

Consider an electron-hole pair q_n, q_p originating on a point x_0 on the center-line of two opposite strips of a double-sided strip detector. The motion of the electron towards the n-electrode x_n is equivalent to the motion of a hole in the opposite direction to the p-electrode x_p. The total induced charge on electrode k after the charges have traversed the detector is

$$Q_k = q_p[\Phi_{Qk}(x_p) - \Phi_{Qk}(x_0)] + q_n[\Phi_{Qk}(x_n) - \Phi_{Qk}(x_0)]$$

since the hole charge $q_p = q_e$ and $q_n = -q_e$

$$Q_k = q_e[\Phi_{Qk}(x_p) - \Phi_{Qk}(x_0)] - q_e[\Phi_{Qk}(x_n) - \Phi_{Qk}(x_0)]$$
$$Q_k = q_e[\Phi_{Qk}(x_p) - \Phi_{Qk}(x_n)]$$

If the signal is measured on the p-electrode, collecting the holes,

$$\Phi_{qk}(x_p) = 1$$
$$\Phi_{qk}(x_n) = 0$$

and $Q_k = q_e$.

If, however, the charge is collected on the neighboring strip $k+1$, then

$$\Phi_{Q(k+1)}(x_n) = 0$$
$$\Phi_{Q(k+1)}(x_p) = 0$$

and $Q_{k+1} = 0$.

In general, if moving charge does not terminate on the measurement electrode, signal current will be induced, but the current changes sign and integrates to zero.

This is illustrated in the following schematic plot of the weighting field in a strip detector (from Radeka)

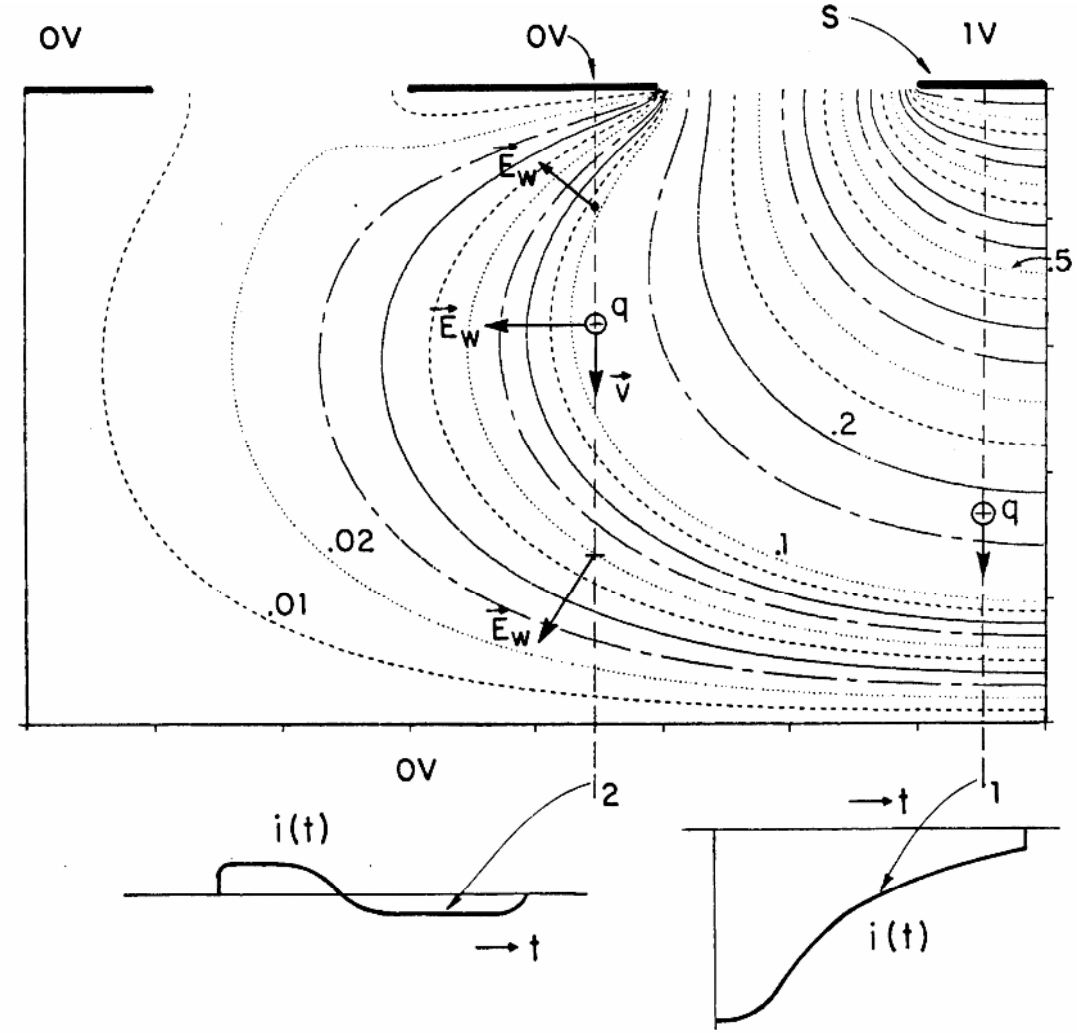

Cuts through the Weighting Field in a Strip Detector
(d= 300 μm, p= 50 μm)

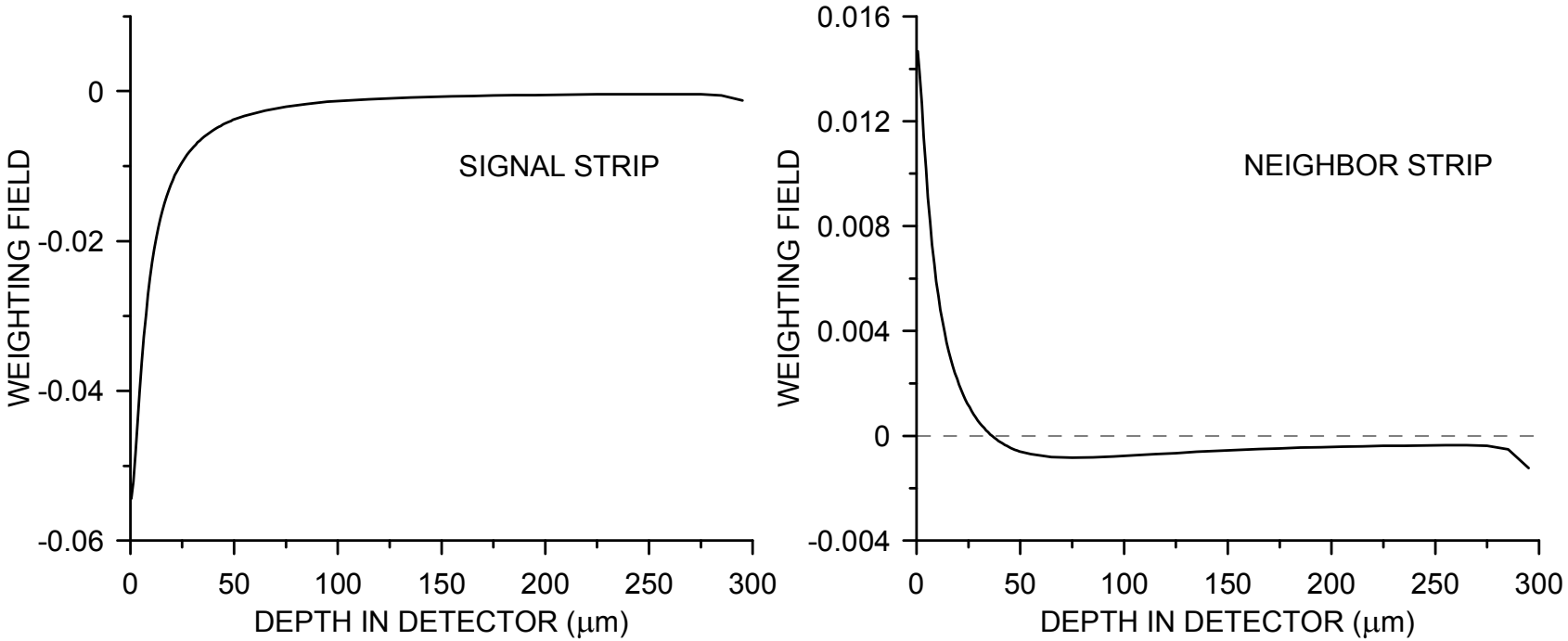

Note, however, that this charge cancellation on “non-collecting” electrodes relies on the motion of both electrons and holes.

Assume, for example, that the holes are stationary, so they don't induce a signal. Then the first term of the first equation above vanishes, which leaves a residual charge

$$Q_k = q_e[\Phi_{Qk}(x_0) - \Phi_{Qk}(x_n)]$$

since for any coordinate not on an electrode

$$Q_k(x_0) \neq 0$$

although it may be very small.

An important consequence of this analysis is that one cannot simply derive pulse shapes by analogy with a detector with contiguous electrodes (i.e. a parallel plate detector of the same overall dimensions as a strip detector). Specifically,

1. the shape of the current pulses can be quite different,

2. the signals seen on opposite strips of a double-sided detector are not the same (although opposite in sign), and

3. the net induced charge on the p- or n-side is not split evenly between electrons and holes.

- Because the weighting potential is strongly peaked near the signal electrode, most of the charge is induced when the moving charge is near the signal electrode.

- As a result, most of the signal charge is due to the charge terminating on the signal electrode.

Current pulses in strip detectors (track traversing the detector)

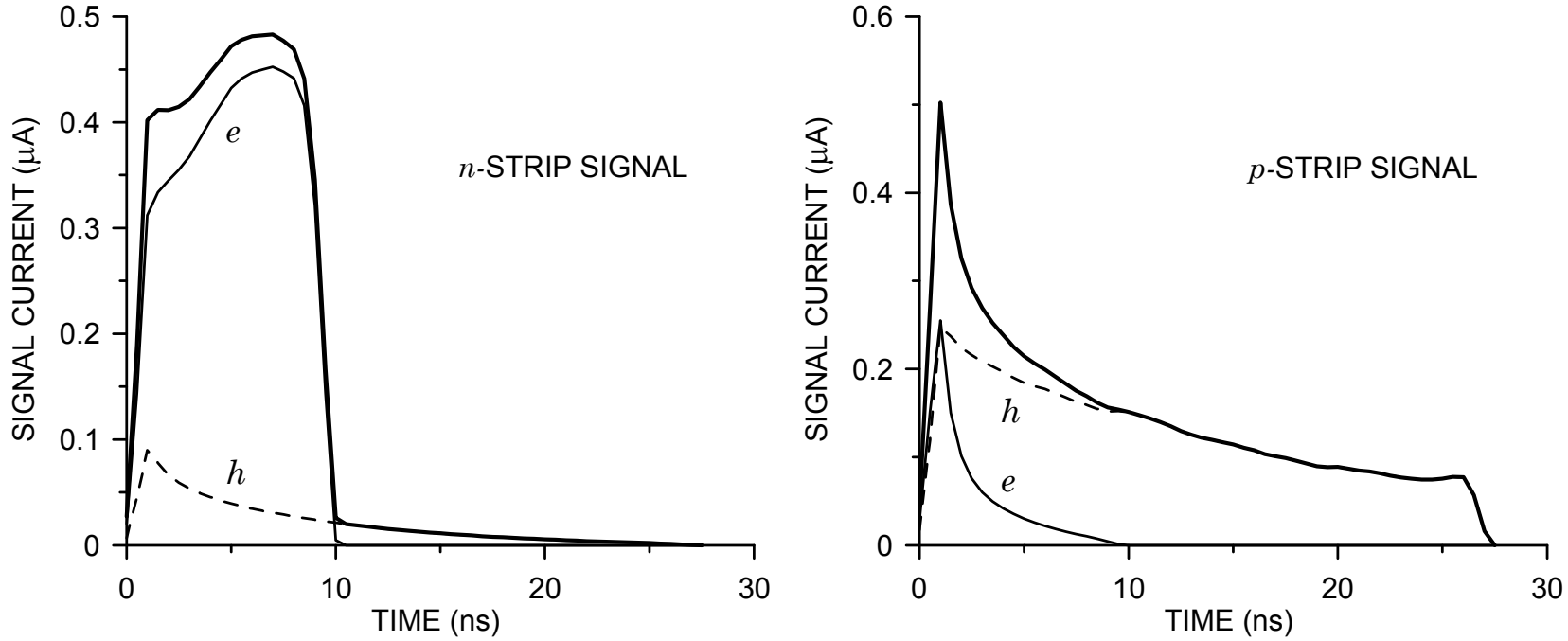

The duration of the electron and hole pulses is determined by the time required to traverse the detector as in a parallel-plate detector, but the shapes are very different.

Strip Detector Signal Charge Pulses

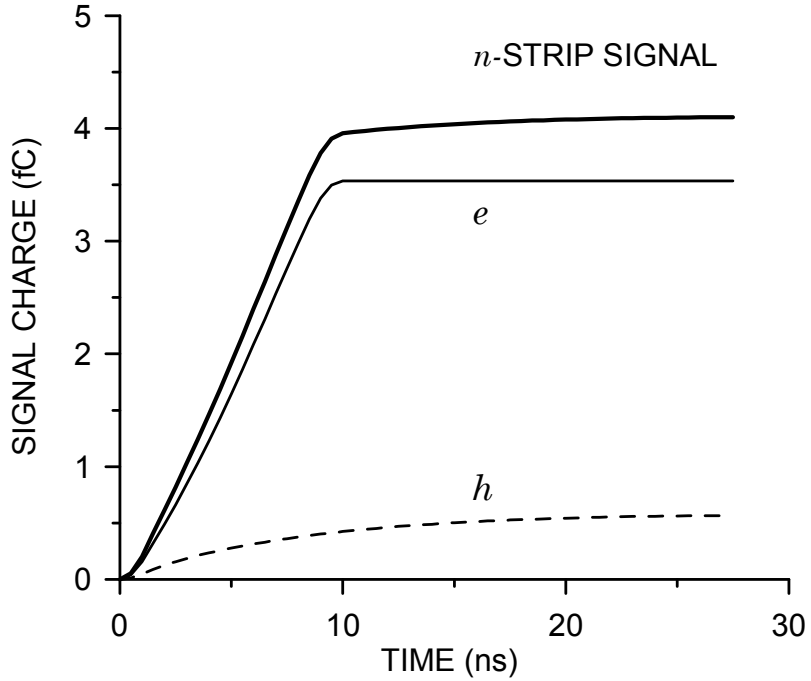

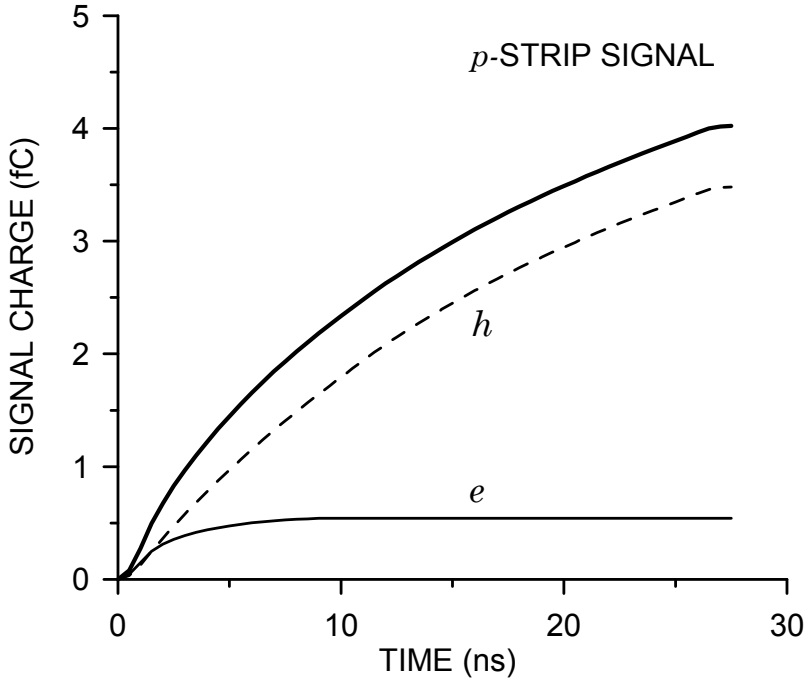

For comparison:

Current pulses in pad detectors (track traversing the detector)

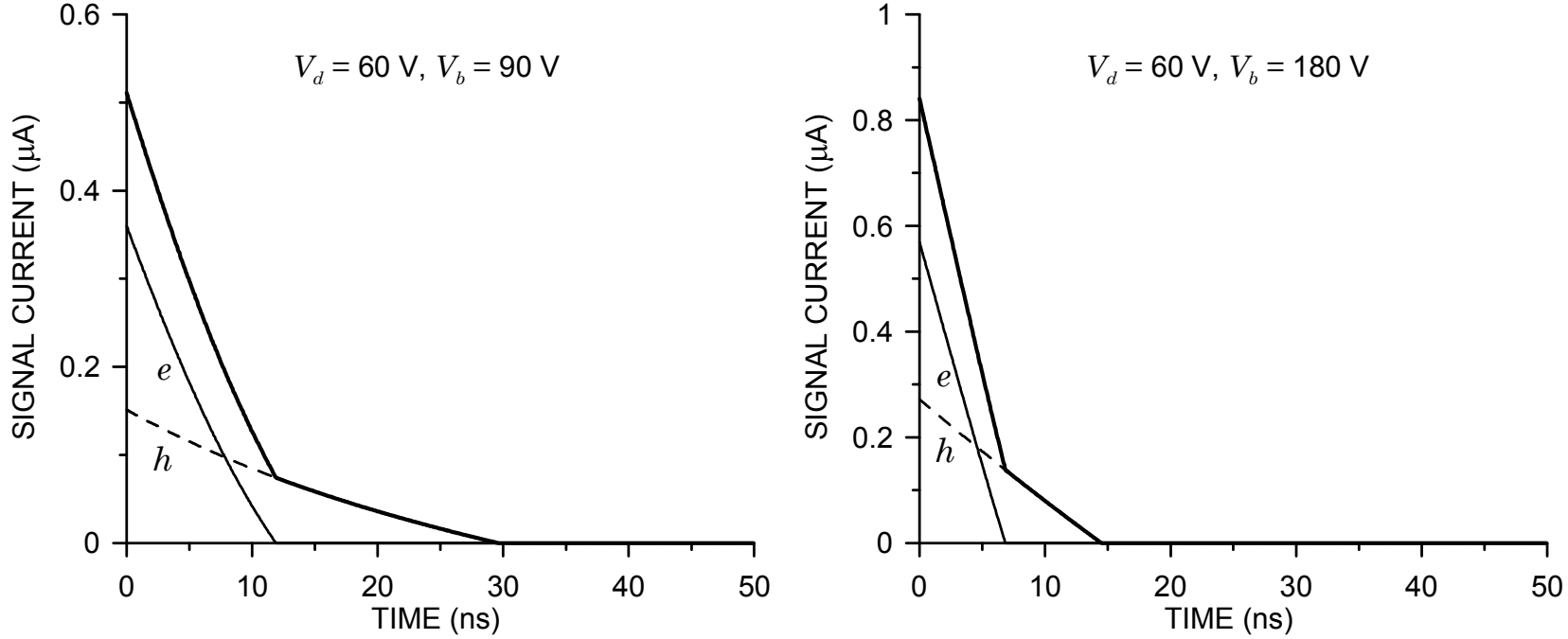

For the same depletion and bias voltages the pulse durations are the same as in strip detectors, although the shapes are very different.

Overbias decreases the collection time.

Operation at or below full depletion leads to long “tails” from the low-field region.

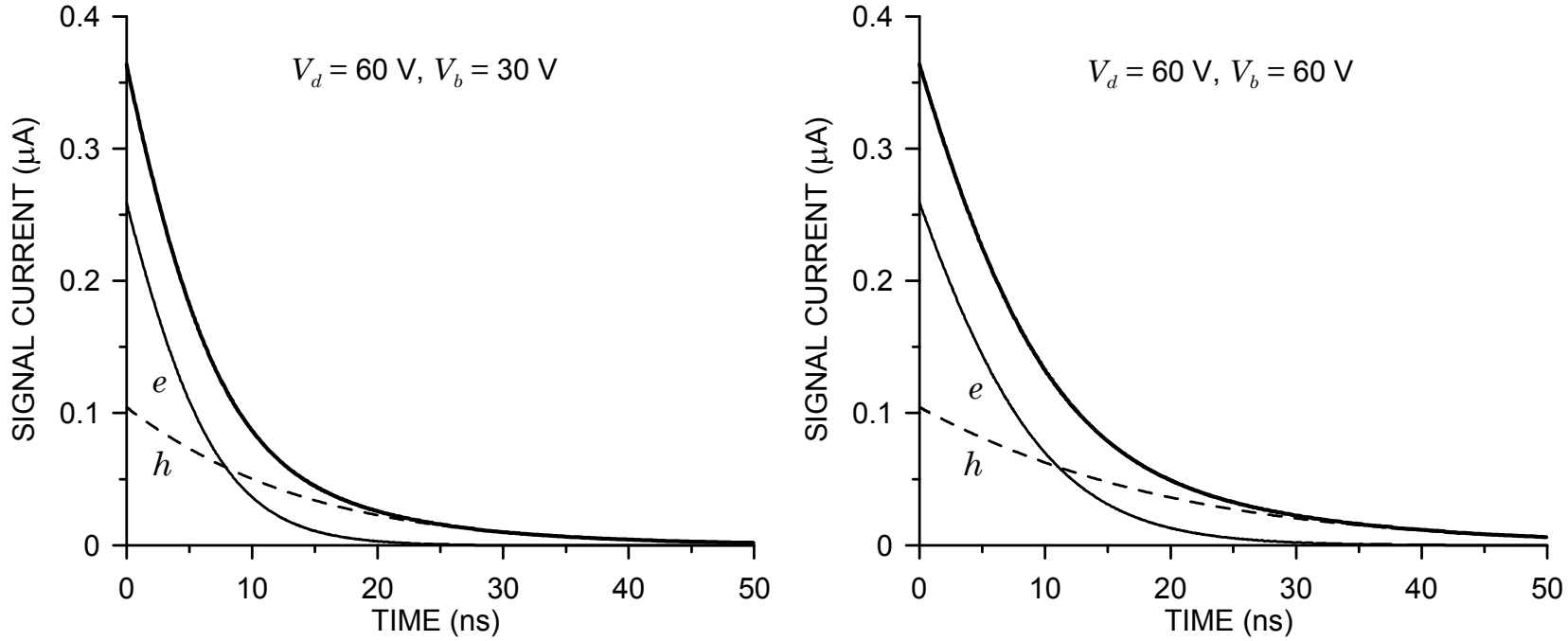

3. Gaseous Detectors (Ionization and Proportional Chambers)

Incident radiation forms electron-ion pairs. In gases the ionization energy is typically ~ 30 eV.

Electrons and ions drift under influence of electric field and induce signal current on detector electrodes.

Velocity is collision limited, so it depends on the electric field and the gas density:

$$v \propto \frac{E}{p},$$

where p is the gas pressure.

Thus the expression for the drift velocity is commonly written as

$$v = \mu E \frac{p_0}{p} = \mu p_0 \frac{E}{p},$$

where the mobility μ is determined at standard pressure p_0.

The drift velocity in gases is often plotted vs. the reduced field E/p.

In reality the collision cross section is energy dependent, so this simple relationship does not hold over the full range of fields (i.e. electron energy).

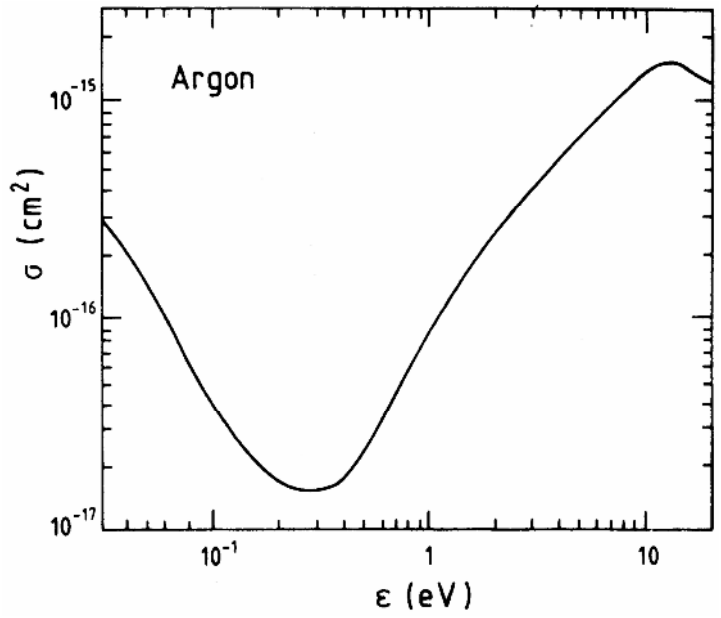

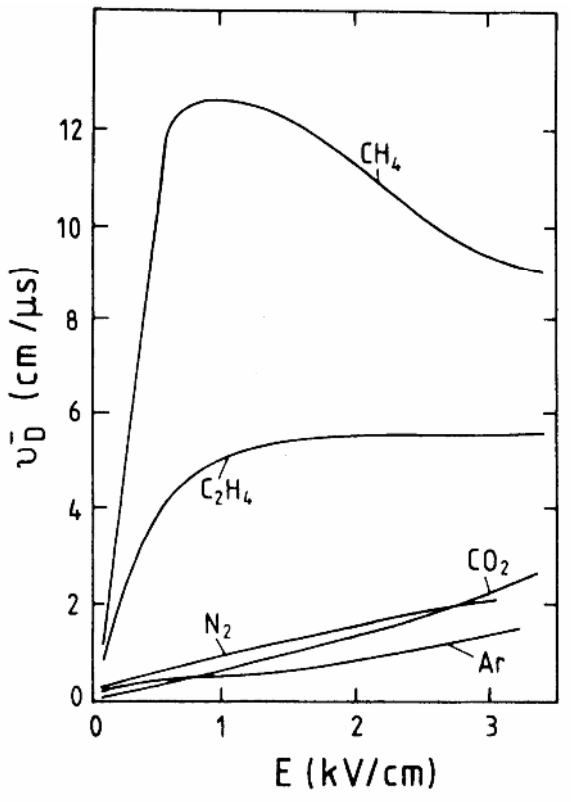

At electron energies ~ 0.1 eV the gas becomes nearly transparent, so acceleration is large, but then decreases at higher electron energies.

Electron velocity vs. drift field for various mixtures of Argon and Isobutane.

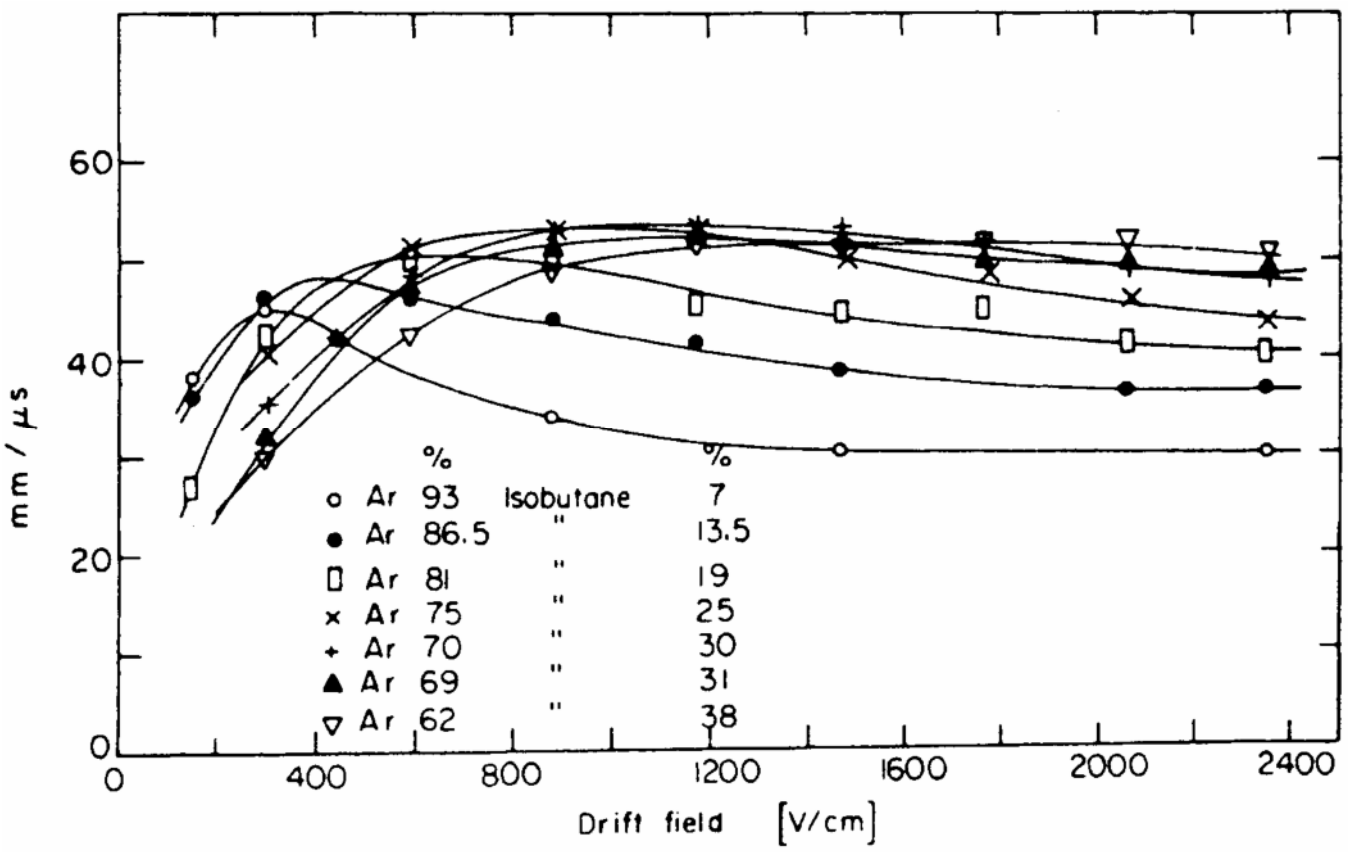

Electrons can be captured by molecules of electronegative gases such as O_2, Cl_2^-, NH_3 and H_2O, leading to a loss in signal.

In gases such as N_2, H_2 and CH_4 capture is negligible, but it is important to control gas purity to avoid deleterious trace contamination by electronegative impurities.

Drift velocity of ions

Measured mobilities of ions in various gases

Gas	Ion	Mobility [cm^2/Vs)
He	He^+	10.2
Ar	Ar^+	1.7
Ar	$(OCH_3)_2CH_2^+$	1.51
Iso-C_4H_{10}	$(OCH_3)_2CH_2^+$	0.55
$(OCH_3)_2CH_2$	$(OCH_3)_2CH_2^+$	0.26
Iso-C_4H_{10}	$IsoC_4H_{10}^+$	0.61
Ar	CH_4^+	1.87
CH_4	CH_4^+	2.26
Ar	CO_2^+	1.72
CO_2	CO_2^+	1.09

At 1 kV/cm ions are of order 1000 times slower than electrons.

3.1. Parallel Plate Ionization Chamber

Consider a simple parallel plate ionization chamber with an electrode spacing of 1 cm, operated at a voltage of 1 kV.

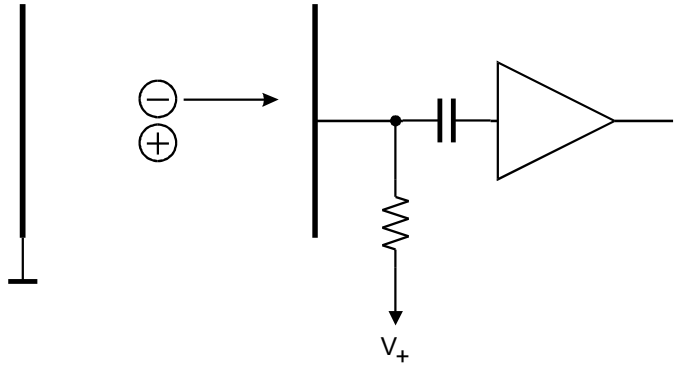

At a field of 10^3 V/cm the electron velocity is typically 10^6 cm/s, whereas the ion velocity is roughly 10^3 cm/s.

Electrons require 1 μs to traverse the full detector volume; the ions take 1000 times longer, i.e. 1 ms.

Assume the integration time of the pulse processor is set to 1 μs, to accommodate the maximum collection of the electrons. Within this time interval the ions will only move

$$\Delta x = v t_{\text{int}} = 10^3 \cdot 10^{-6} = 10^{-3} \text{ cm}$$

so the induced charge

$$\Delta Q = N q_e \frac{\Delta x}{d} = 10^{-3} N q_e$$

Since the induced charge due to electrons can range from 0 to Nq_e, depending on the origin of the electron-ion pair, the obtainable energy resolution will be much worse than expected from the statistics of electron-ion formation.

The position dependence of the induced charge can be eliminated (practically) by introduction of a shielding grid (Frish grid).

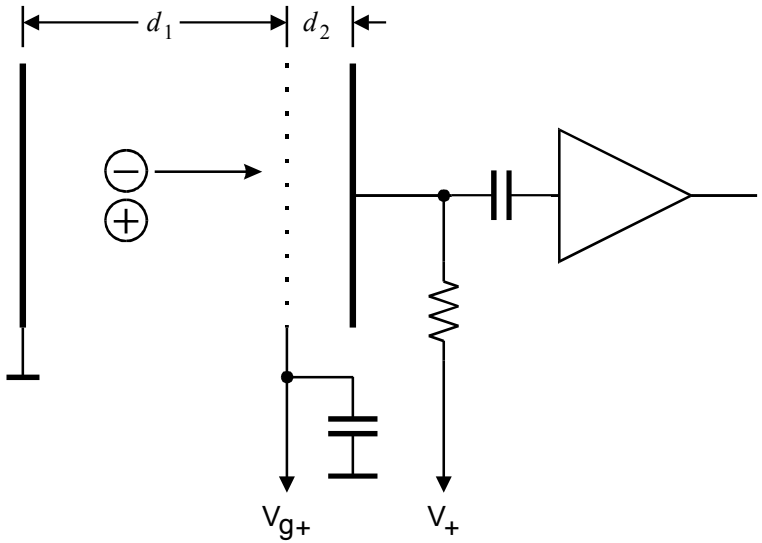

Charges moving in the space d_1 between the grid and the left electrode induce current on these two electrodes, but not on the signal electrode.

When electrons move into the region d_2 between the grid and the signal electrode, they induce current on the signal electrode.

The two regions d_1 and d_2 constitute separate volumes for induced currents, i.e. the induced currents flow in two distinct loops.

Depending on the point of origin, the electrons drifting induce the charge

$$\Delta Q_1 = N q_e \frac{\Delta x}{d_1}$$

in the circuit defined by the left electrode and the grid. However, all electrons passing through the grid and traversing the region d_2 will induce

$$\Delta Q_2 = N q_e \frac{d_2}{d_2} = N q_e$$

in the circuit defined by the grid and the signal electrode, so the full signal charge is induced for all charges originating in the region d_1.

If the grid is made sufficiently dense to be an effective electric shield, will the electrons still pass through it?

By appropriate choice of geometry and grid potential the efficiency of electron transmission can be ~100%.

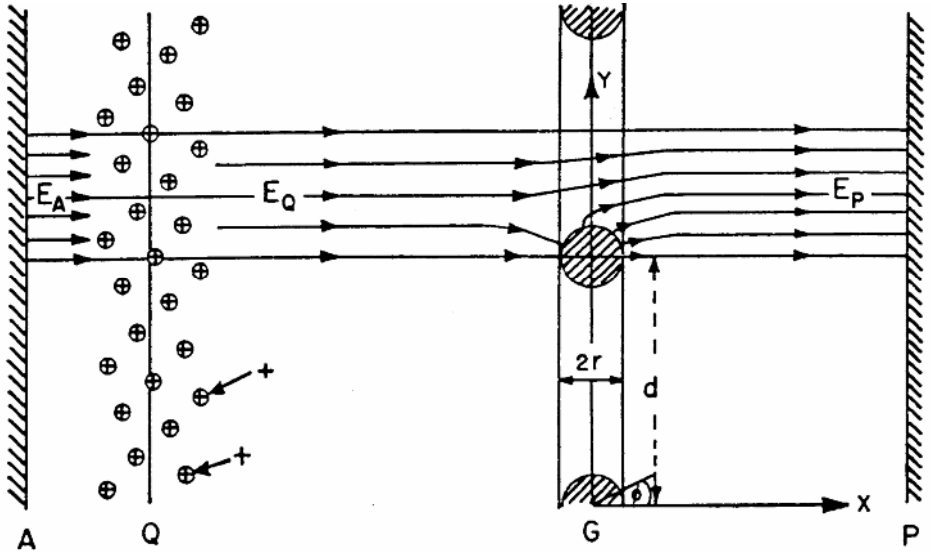

Inefficiency of shielding σ vs. wire radius/pitch r/d and ratio of pitch to grid position d/p (p is d_2 on the previous page).

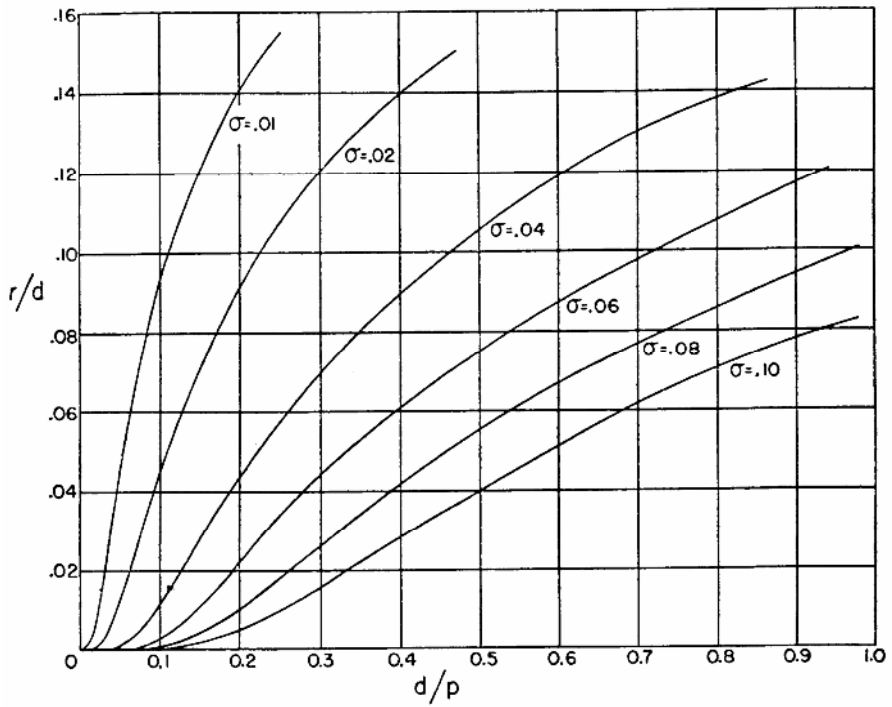

Rather dense grids are needed for good shielding.

By increasing the potential between the grid G and the collection electrode P such that the field E_P is greater than E_Q, the grid can be made increasingly transmissive for electrons. Depending on the grid geometry, ratios $E_P/E_Q \approx 2 – 3$ will provide ~100% transmission

(Bunemann et al., Canadian J. of Res. **27A** (1949) 191

3.2. Proportional Chambers

At high electric fields electrons can acquire sufficient energy between collisions to ionize gas molecules. As discussed for photodiodes, this mechanism can be exploited to increase the signal from the detector.

The probability of ionization is determined by the “first Townsend coefficient” α. The increase in the number of electrons traversing an increment dx is

$$dN = N\ \alpha\ dx$$

In a uniform electric field the signal gain over a distance L is

$$G = \frac{N}{N_0} = e^{\alpha L}$$

High fields are typically obtained by utilizing the radial dependence of the electric field near a thin wire.

In a coaxial geometry with an applied voltage V_b the field

$$E(r) = \frac{V_b}{r \ln \frac{r_2}{r_1}} ,$$

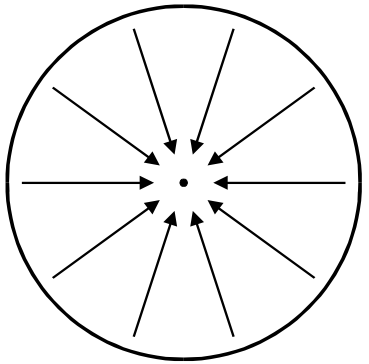

where r_1 is the inner and r_2 the outer radius.

Typical wire diameters for the inner conductor are 25 – 50 μm.

If the gas gain is to be the same for all signals, the volume of the multiplication region must be negligible compared to the total detection volume.

Assume that the field required for the onset of appreciable ionization is 50 kV/cm ("critical field"). The radius at which appreciable ionization sets in is

$$r_c = \frac{V_b}{E_c \ln \frac{r_2}{r_1}}$$

If the wire diameter is 25 μm and the outer radius is 25 mm, with a bias of 1 kV applied to the chamber, the critical radius is about 30 μm.

$\Rightarrow$ The avalanche region is about 10^{-6} of the chamber volume.

Induced Signal

The avalanche forms both electrons and ions. The electrons drift towards the inner wire and the ions towards the outer electrode.

The electrons only drift a short distance (10s of μm), but the $1/r$ dependence of the weighting field increases their contribution.

Assume N electrons and ions formed at radius r. The weighting potential for the induced charge is

$$\Phi_Q = \int F(r)dr = \frac{1}{\ln(r_2/r_1)}\int \frac{1}{r}dr = \frac{\ln r}{\ln(r_2/r_1)},$$

so the induced charge due to electrons and ions

$$Q_{s,el} = -Nq_e\left(\Phi_Q(r_1) - \Phi_Q(r)\right) = Nq_e\frac{\ln(r/r_1)}{\ln(r_2/r_1)}$$

$$Q_{s,ions} = Nq_e\left(\Phi_Q(r_2) - \Phi_Q(r)\right) = Nq_e\frac{\ln(r_2/r)}{\ln(r_2/r_1)}$$

The ratio of induced charges $$\frac{Q_{s,el}}{Q_{s,ions}} = \frac{\ln(r/r_1)}{\ln(r_2/r)}$$

Since the avalanche builds up within 10s of microns of the inner conductor $r/r_1 < 2$, whereas r_2/r is of order 1000

$$\frac{Q_{s,el}}{Q_{s,ions}} < \frac{\ln(2)}{\ln(1000)} = 0.1$$

The total charge signal is dominated by the motion of the ions.

However, since the induced current

$$i_s = Nq_e v(r) F(r) = Nq_e \mu(E)\ E(r)\ F(r)$$

$$i_s = Nq_e \mu(E) \frac{V}{(\ln(r_2/r_1))^2} \frac{1}{r^2} \propto \frac{\mu(E)}{r^2}$$

the electron current is orders of magnitude greater than the ion current, due to the greater mobility of the electrons and the fact that they are moving at very small radii.

Hence, the signal current has a fast and large component due to the electrons superimposed on the ion current, which is much smaller, but orders of magnitude longer.

Since the electron component may be less than 1 ns in duration, very fast electronics and low-inductance chamber design are needed to utilize (or even see) it.

The long drift time of the ions limits the rate capability of proportional chambers.

At high rates the accumulated space charge from the ions distorts the electric field and reduces the gain.

The use of small gas volumes that restrict the maximum ion drift distance increases the rate capability.

Example: “straw” tubes with an outer diameter of several mm allow rates of $>10^7$ s^{-1}.

3.3 Position Sensitive Detectors

1. Multi-Wire Proportional Chamber (MWPC)

An array of many thin wires forms a multi-channel proportional chamber.

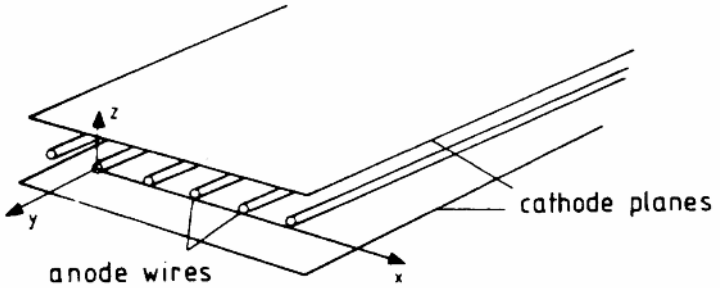

Electrode configuration and field distribution

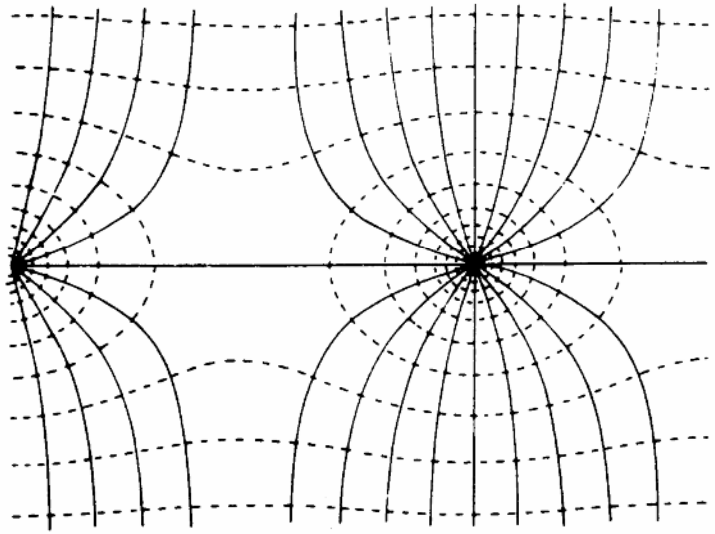

The field near the wires depends primarily on the wire radius.

Many cathode geometries possible.

MWPCs are often used with simple threshold discrimination, where the presence of a “hit” (signal above threshold) indicates the location of a particle.

The integration time of the pulse processing preceding the threshold discriminator determines the fraction of the signal charge that is registered.

Dependence of efficiency vs. integration time (“gate”) and applied voltage.

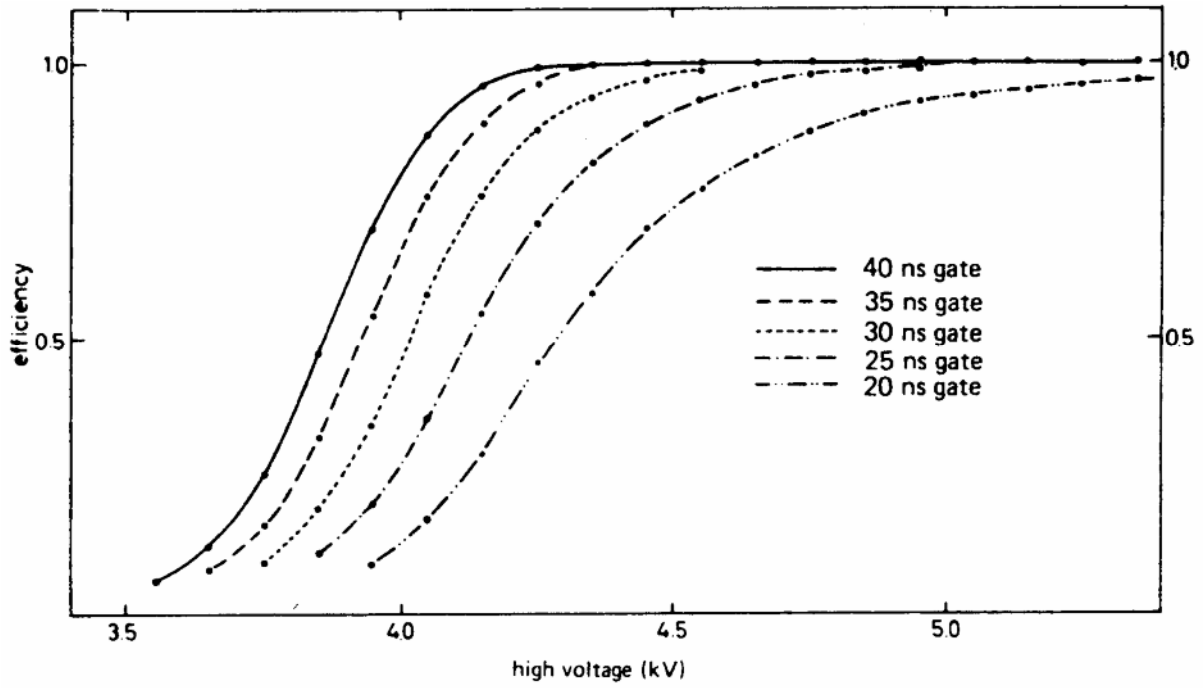

The cathode planes can be segmented to provide additional position sensing.

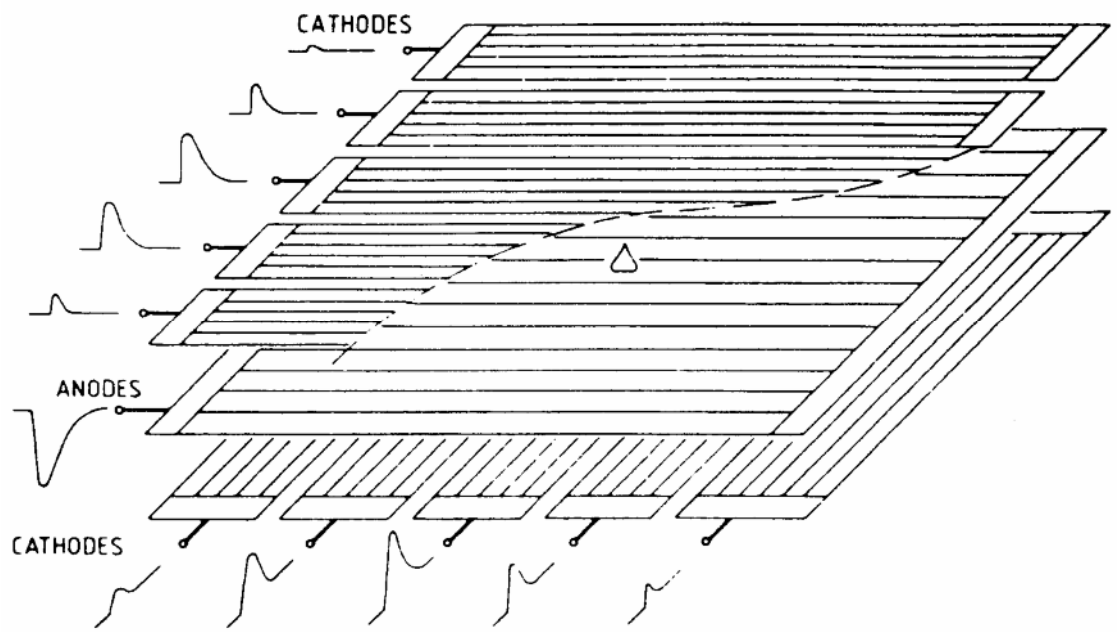

(from Charpak)

The lower cathode plane provides position sensing along the wires.

Evaluation of the pulse height distribution allows interpolation to better than the pitch of the cathode pads.

2. Drift Chambers

In systems where an external time reference is available, the time required for primary charges to reach the avalanche region can be used for position sensing.

Example: “straw” chamber

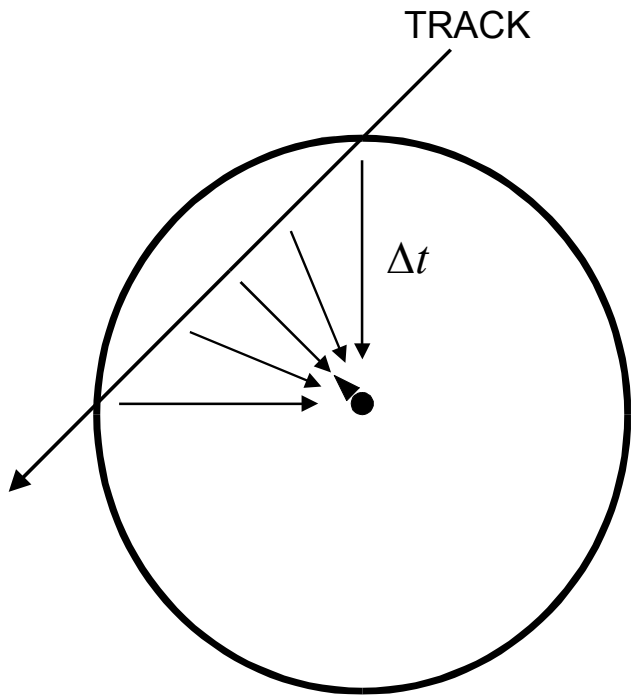

Electrons formed along the track drift towards the central wire.

The first electron to reach the high-field region initiates the avalanche, which is used to derive the timing pulse.

Since the initiation of the avalanche is delayed by the transit time of the charge from the track to the wire, the time of the avalanche can be used to determine the position.

Achievable position resolutions are ~100 μm.

Minimum ionizing particles deposit energy in clusters along the track, so the point of minimum distance does not necessarily coincide with a cluster.

⇒ Pulses have significant time structure (trigger on first pulse)

Top: measured

Bottom: simulated

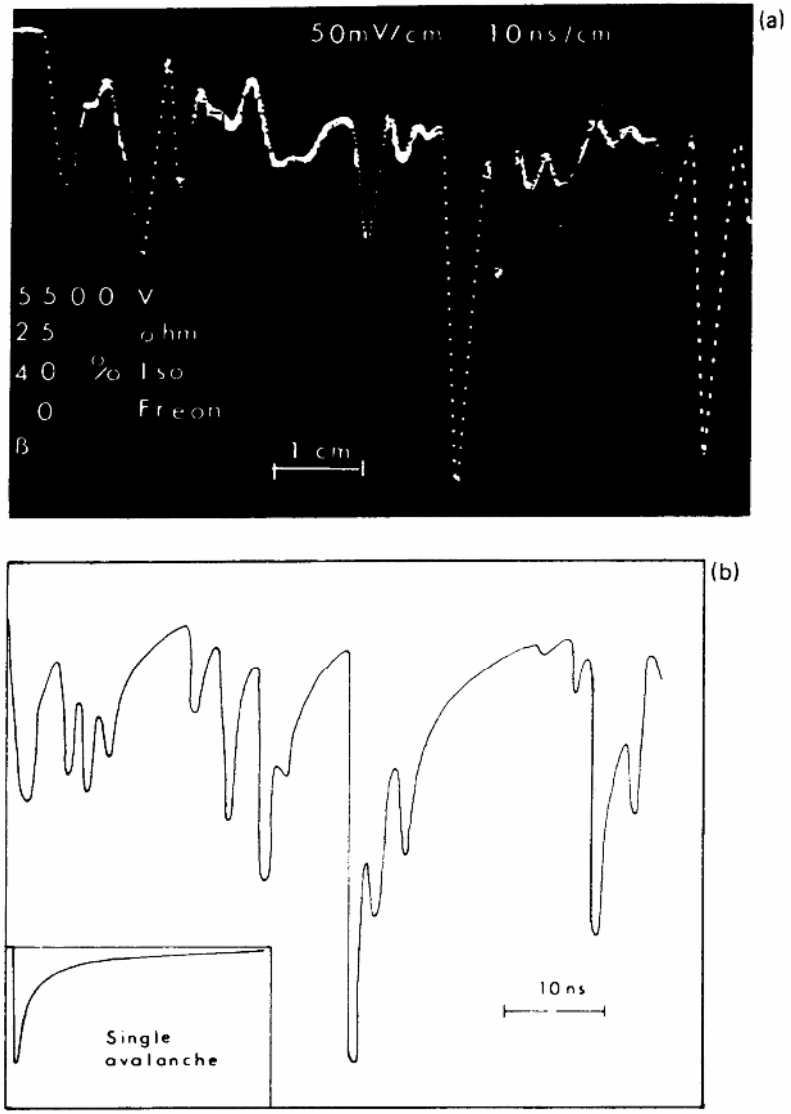

3. Time Projection Chamber (TPC)

The TPC utilizes the principle of a drift chamber on a large scale to provide 3D imaging.

Electrons drift through a large volume to the endcaps, where they avalanche at a grid of wires.

The drift time provides the longitudinal coordinate,

The wires the radial coordinate.

Pads arranged along the wires provide the φ coordinate.

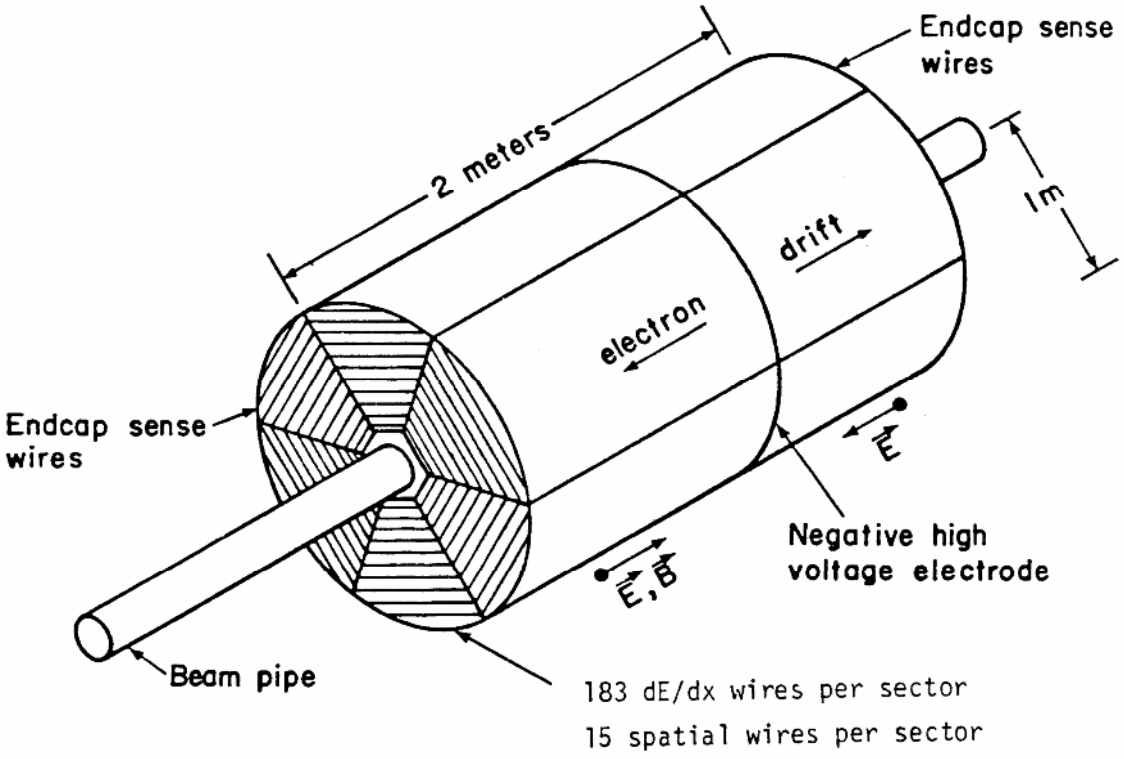

(M.D. Shapiro, thesis, 1984)

Detail of endcap sector

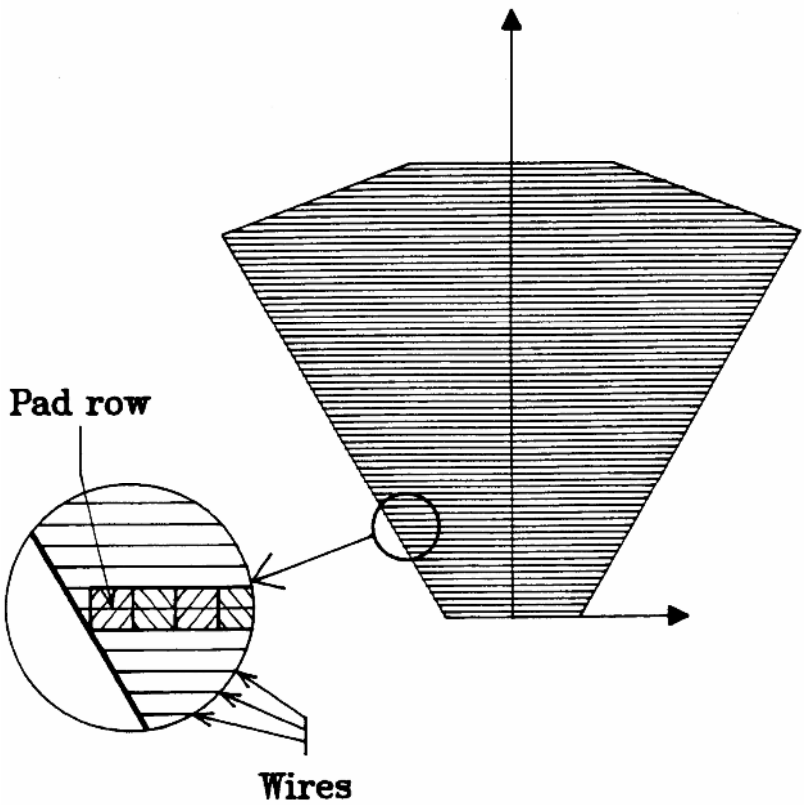

A combination of grids provides
field shaping
avalanching
signal sensing

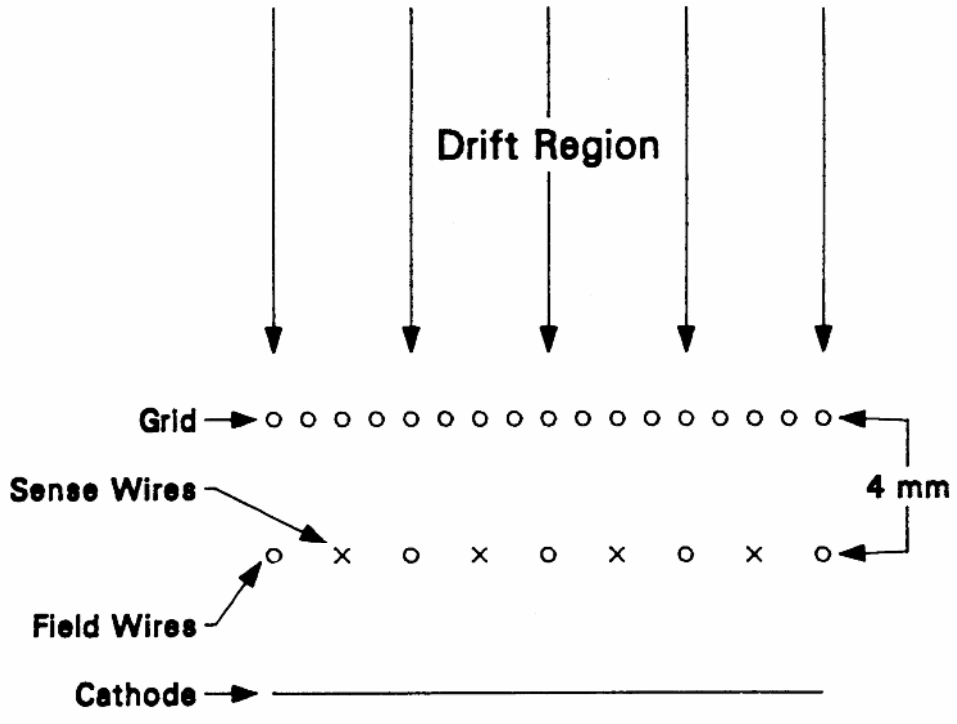

The cathode plane is segmented with rows of pads along the avalanche wires to provide position resolution along the wires.

Analog interpolation improves the resolution in both coordinates.

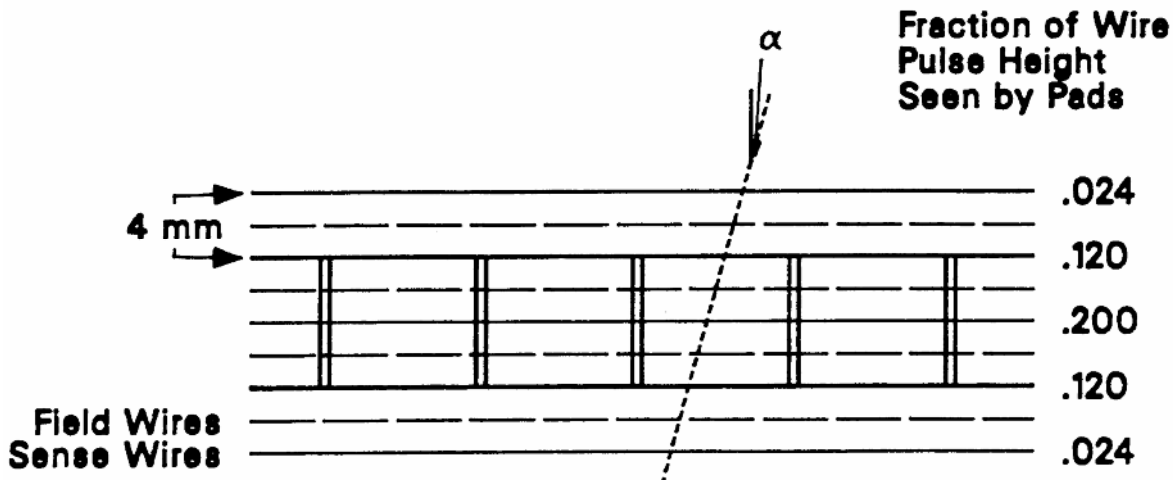

The projection of a particle track on the endcap together with the longitudinal drift time provides true 3D space points.

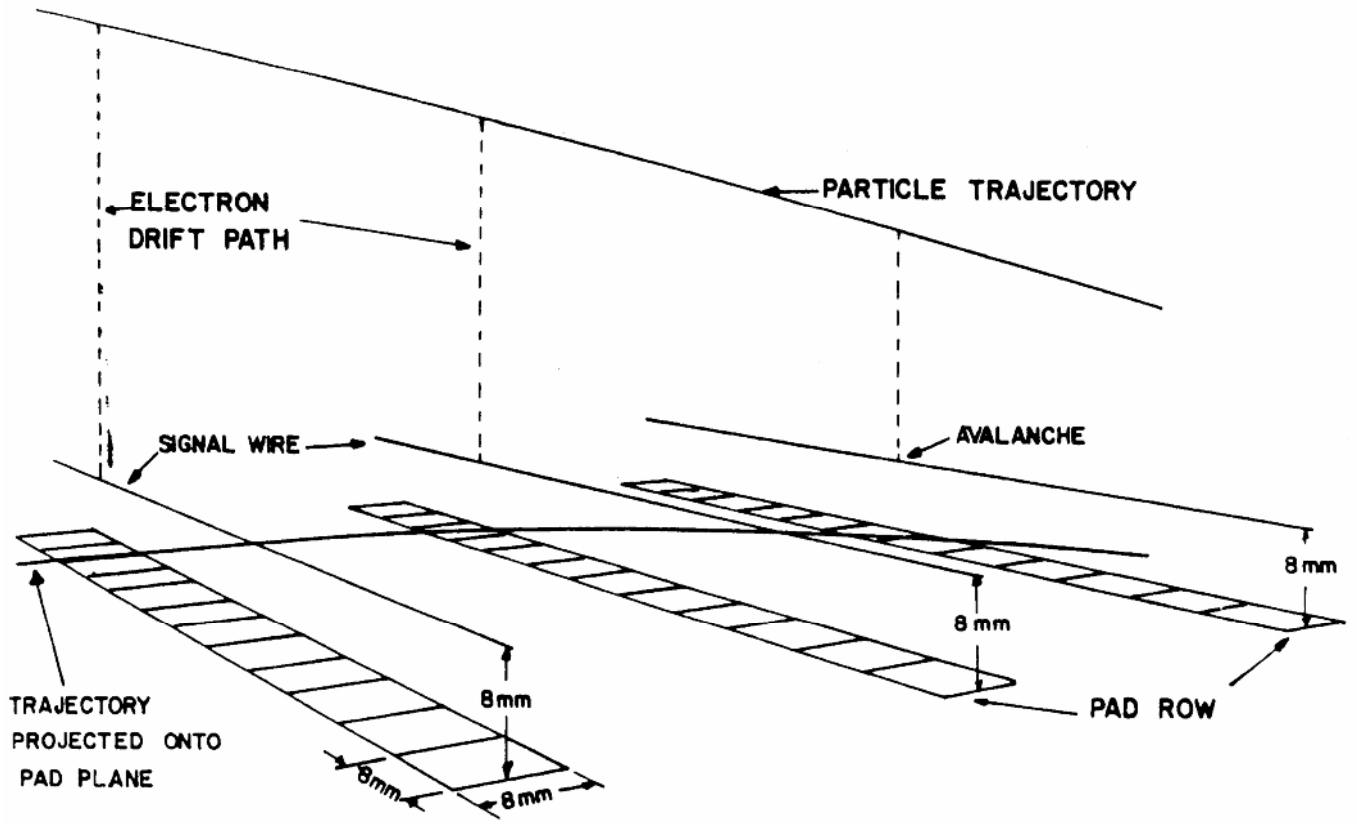

At first glance this device would seem to be unworkable, as transverse diffusion will spread the charge radially with a Gaussian distribution

$$n(r) = \left(\frac{1}{\sqrt{4\pi Dt}} \right)^3 \exp\left(-\frac{r^2}{4Dt} \right)$$

The standard deviation after drifting a distance x $\qquad \sigma_r = \sqrt{Dt} = \sqrt{\frac{2\varepsilon_k x}{q_e E}}$

where e_k is a characteristic energy of the electron ($> (3/2)k_B T$)

The long drift times (10s of μs) would ruin the r and $r\varphi$ resolution.

The key insight (D. Nygren) was that a magnetic field parallel to the electric drift field reduces transverse diffusion.

The transverse diffusion coefficient is reduced by a factor $\qquad \frac{1}{1+\omega^2\tau^2}$,

where $\omega = \frac{q_e B}{m}$ is the cyclotron frequency of the electrons and τ is the mean time between collisions.

For a primary signal cluster with > 150 el the spatial resolution after 1 m drift at $B \approx 1$ T can be < 200 μm.

Example of a large TPC: Aleph detector at CERN.

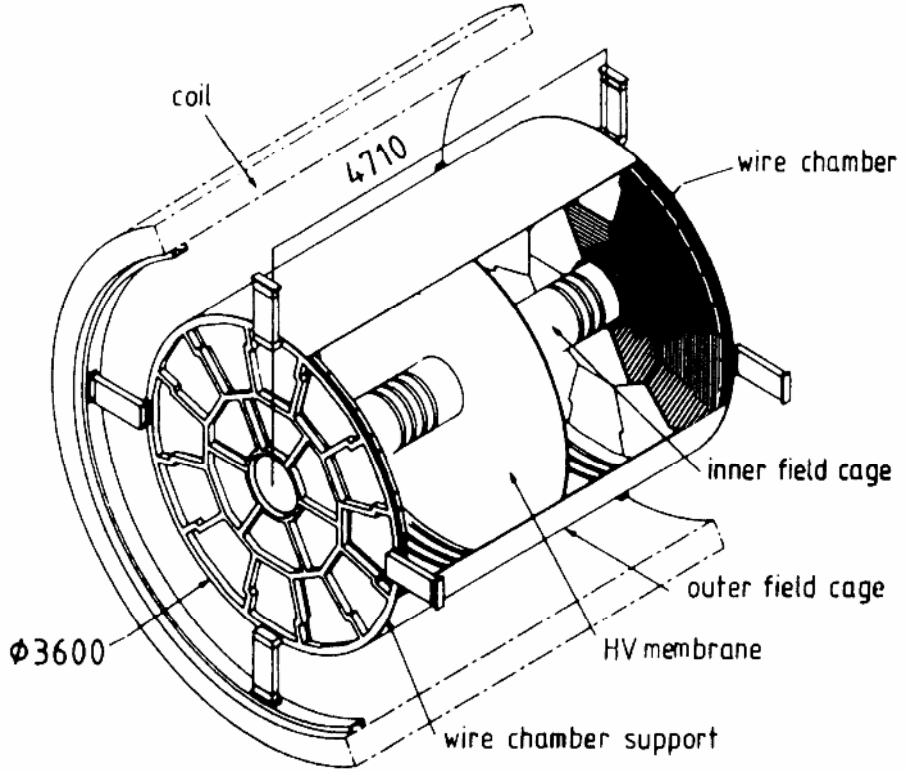

Typical event display

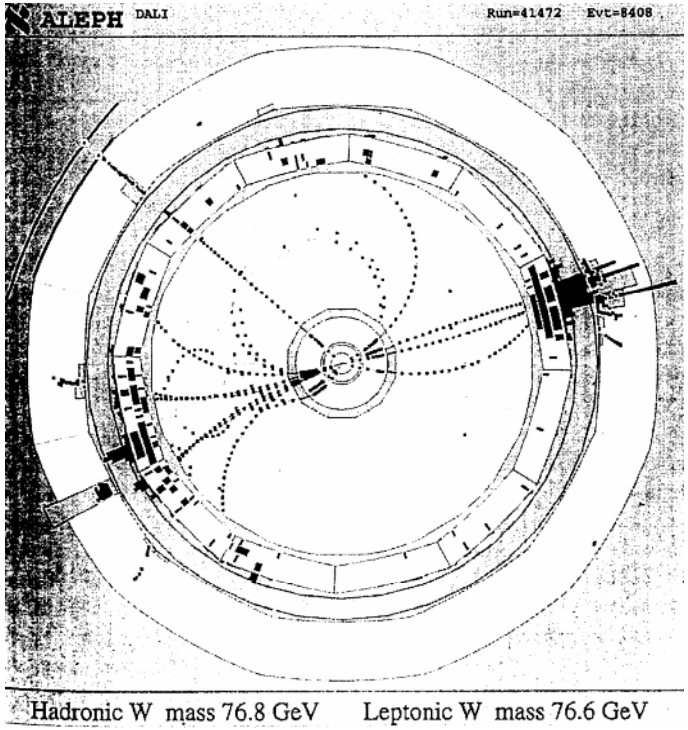

Rate limitations due to ion charge buildup can be mitigated by reducing the cell size. One of the advantages of Si is that characteristic dimensions are microns rather than mm.

Recent developments in proportional chambers utilize technology from semiconductor fabrication to make micron-scale structures.

4. Micro-Strip Gas Chamber (MSGC)

MSGCs utilize strip anodes and cathodes on an insulating substrate.

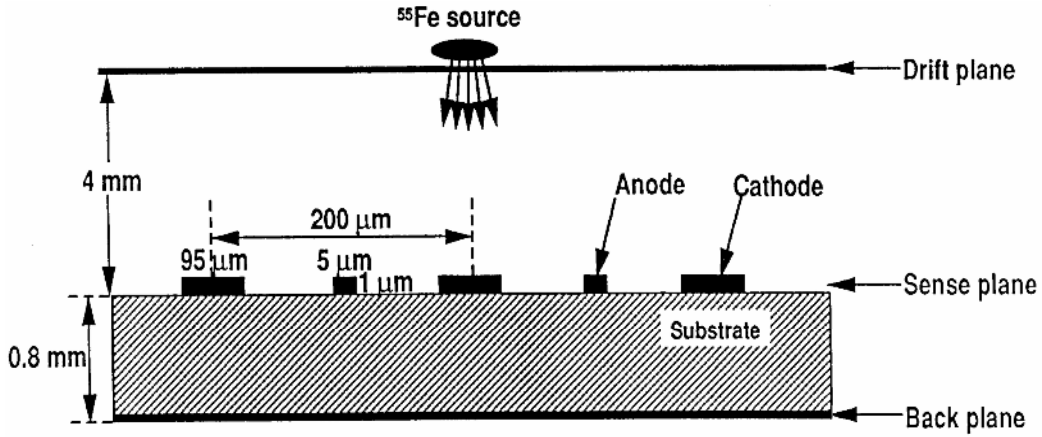

Electrons avalanche at the high field formed at the anode strips.

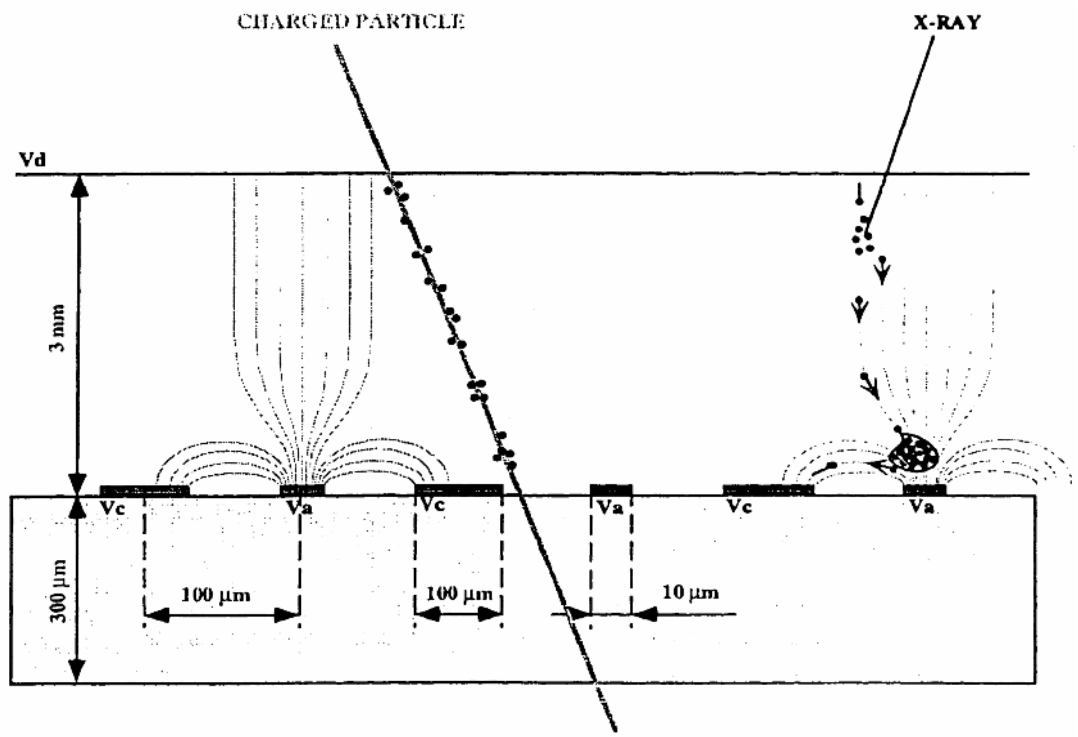

(from Hoch)

The electrodes are fabricated on a glass substrate using standard microfabrication techniques (photolithography + etching).

The properties of the substrate are critical:

If it is perfectly insulating, charge builds up on the surface and changes the field.

Too large a surface conductivity will lead to excessive leakage current.

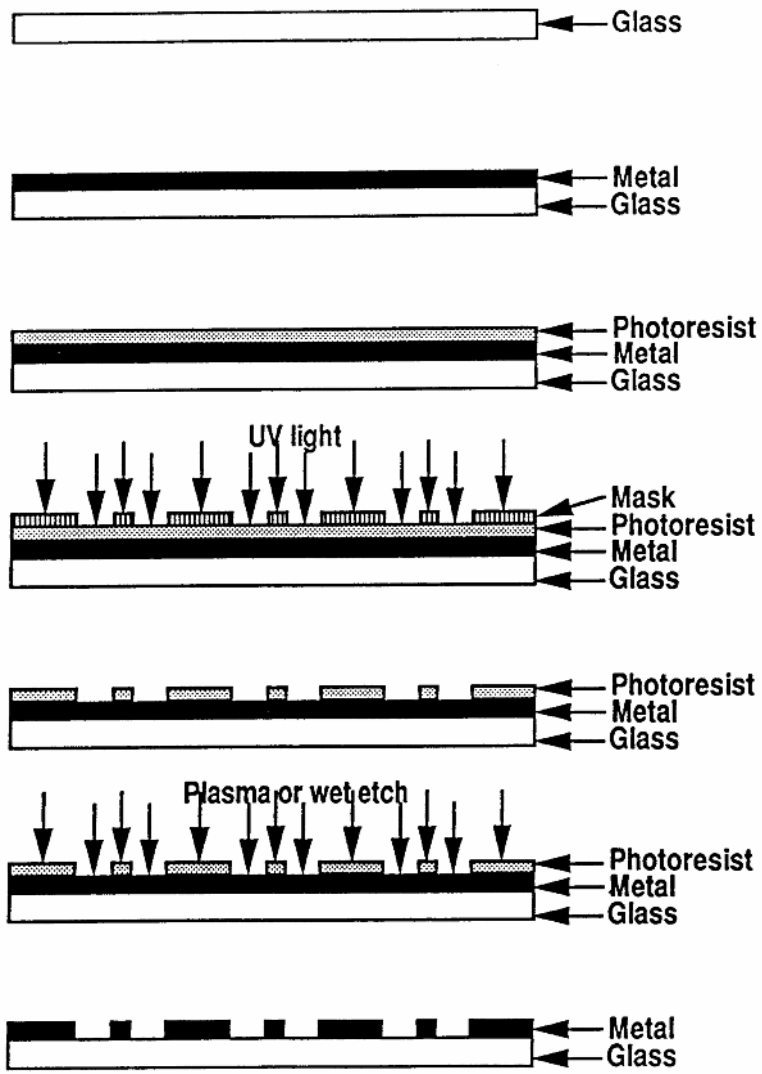

Since the distance between the anode and cathode is much smaller than in conventional wire chambers, the ions are collected more quickly.

Electric field distribution

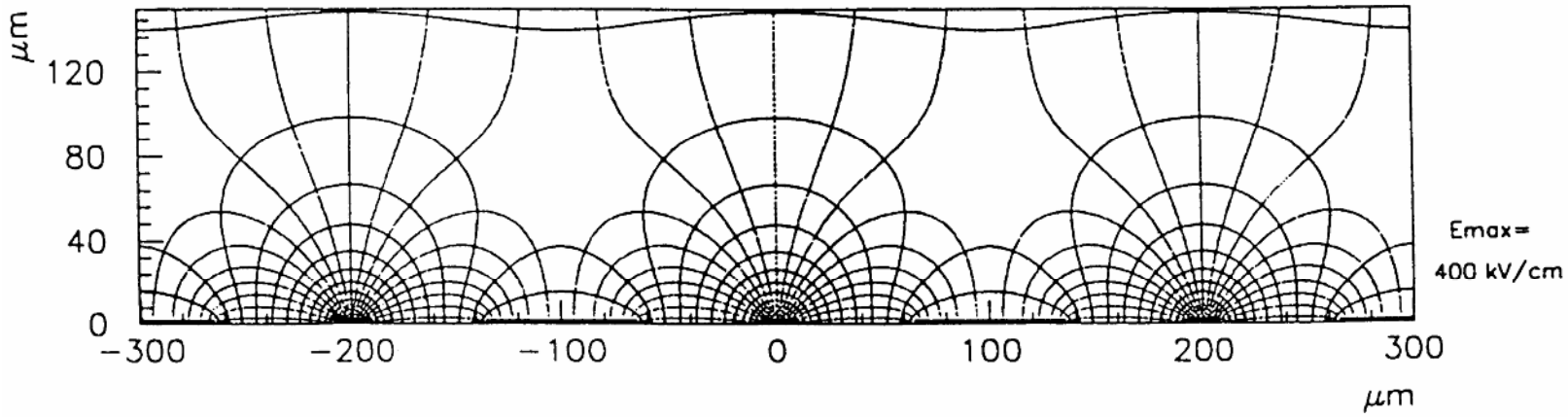

(from Bellazzini)

Because of the faster collection of the ions, the rate capability of an MSGC is superior to that of a multi-wire proportional chamber.

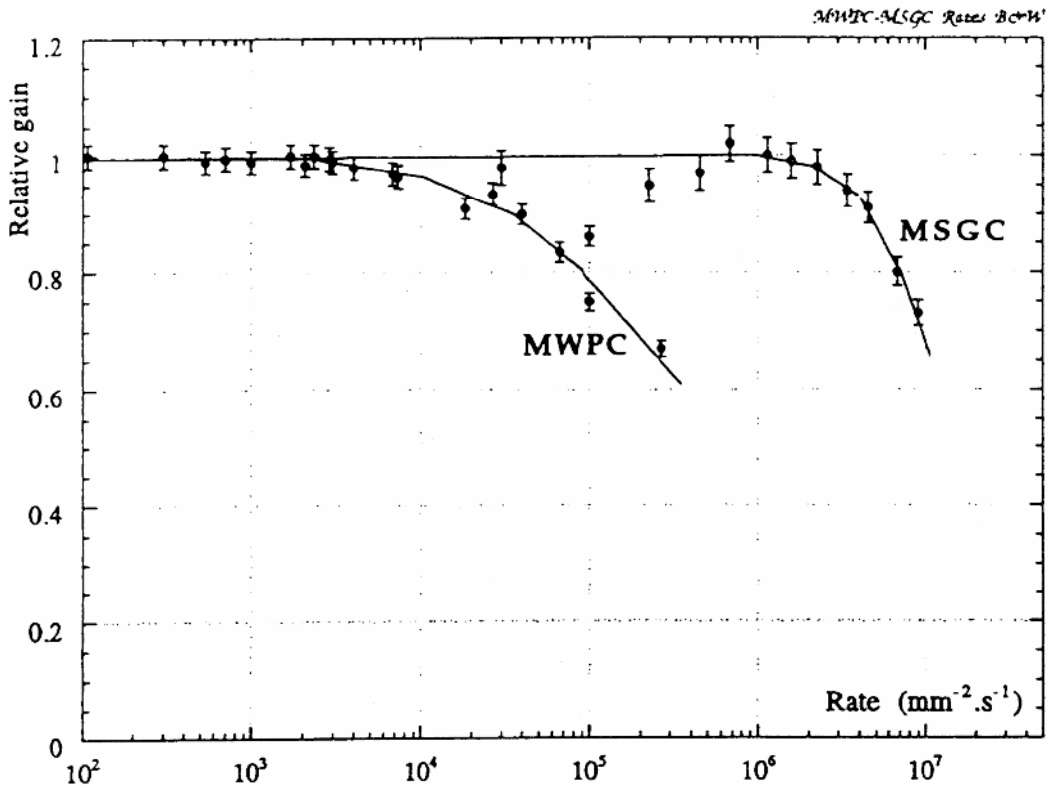

(from Sauli)

Proportional chambers are subject to two critical failure mechanisms:

1. Damage to a strip after sparking

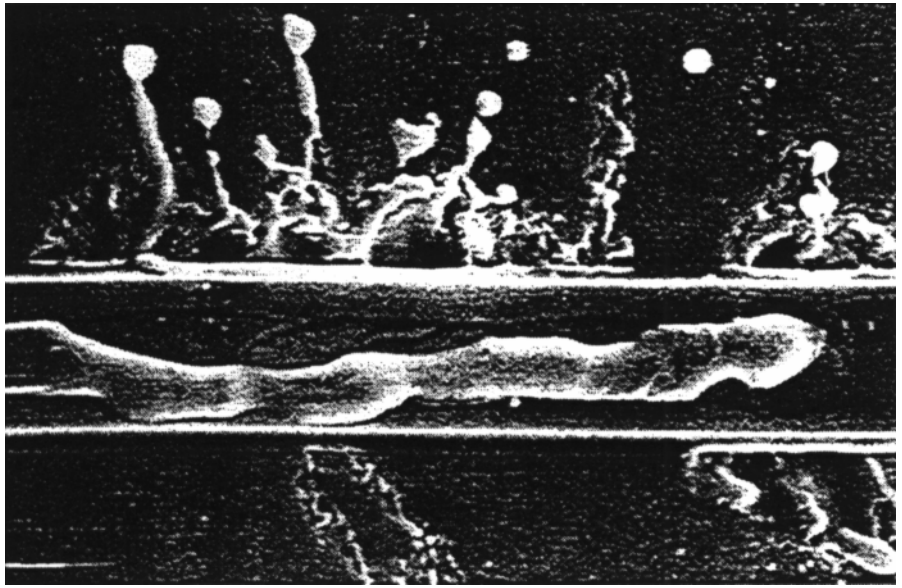

This is an aluminum strip. Metals with higher melting points (e.g. tungsten) improve the resistance to damage from local discharge.

Sharp corners also form local high fields, so the electrodes must be rounded at the ends and corners. Important not to run at higher gain than necessary.

2. Aging

At high fields the hydrocarbons in many gases polymerize on the wires of MWPCs and strips of MSGCs, forming “whiskers” or “droplets” on the electrode. These deposits alter the field distribution and reduce detection efficiency with time.

Judicious choice of gas mixtures and operating conditions (especially low gas gain) can greatly alleviate this problem.

For a review see J. Kadyk, NIM A300(1991)436

5. Micro-Gap Chamber (MGC)

The micro-gap chamber reduces the path for ion collection even more.

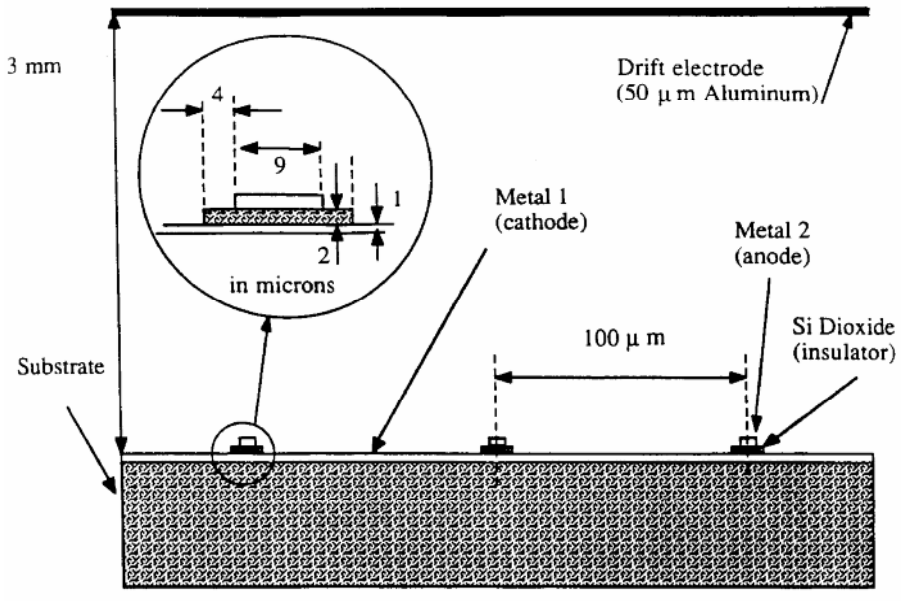

(from Bellazzini)

The cathode is a contiguous metal plane. The anodes are strips placed at a small distance (~2 microns) above the cathode plane, using thin strips of silicon-dioxide.

Field distribution

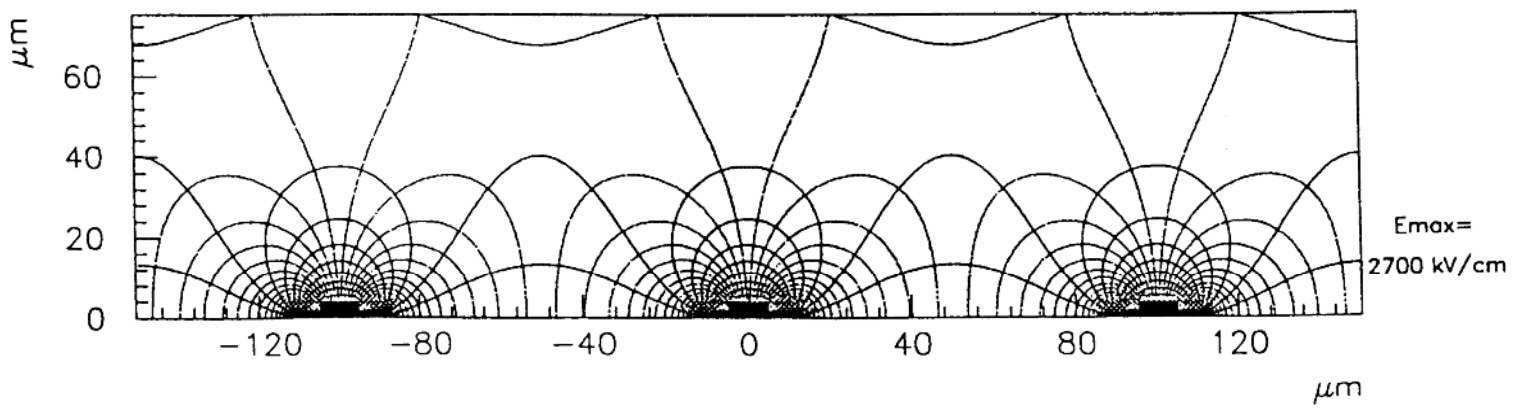

(from Bellazzini)

This geometry eliminates the problem of surface charging.

The rate capability improves because the ions are collected within 10s of microns.

These improvements come at the expense of added fabrication complexity.

6. The Gas Electron Multiplier (GEM)

The gas electron multiplier a gain stage that can be combined with a variety of readout electrode structures.

The GEM consists of two electrodes formed by metal layers on both sides of a thin insulator (typically Kapton).

Perforations in this sandwich form local high field regions in which electrons avalanche in a gas.

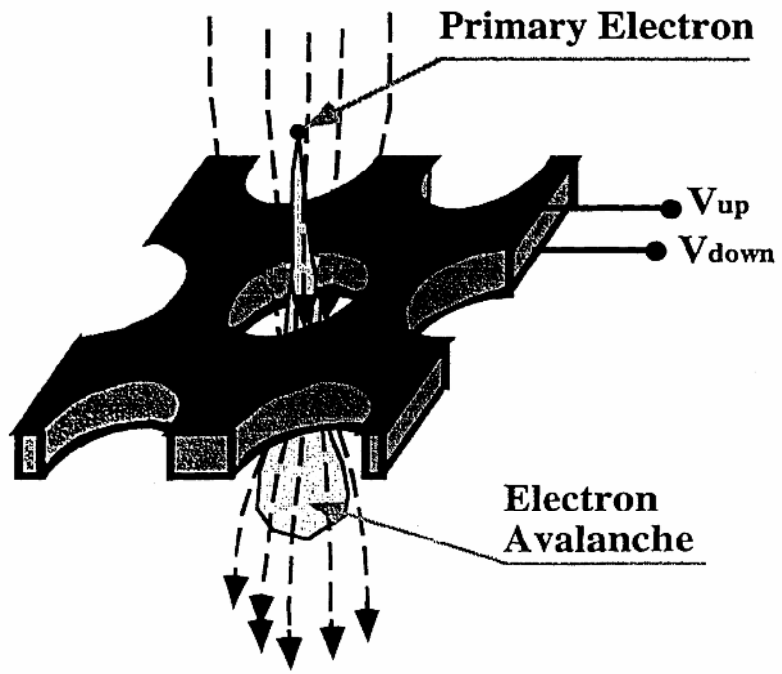

Field distribution in the aperture

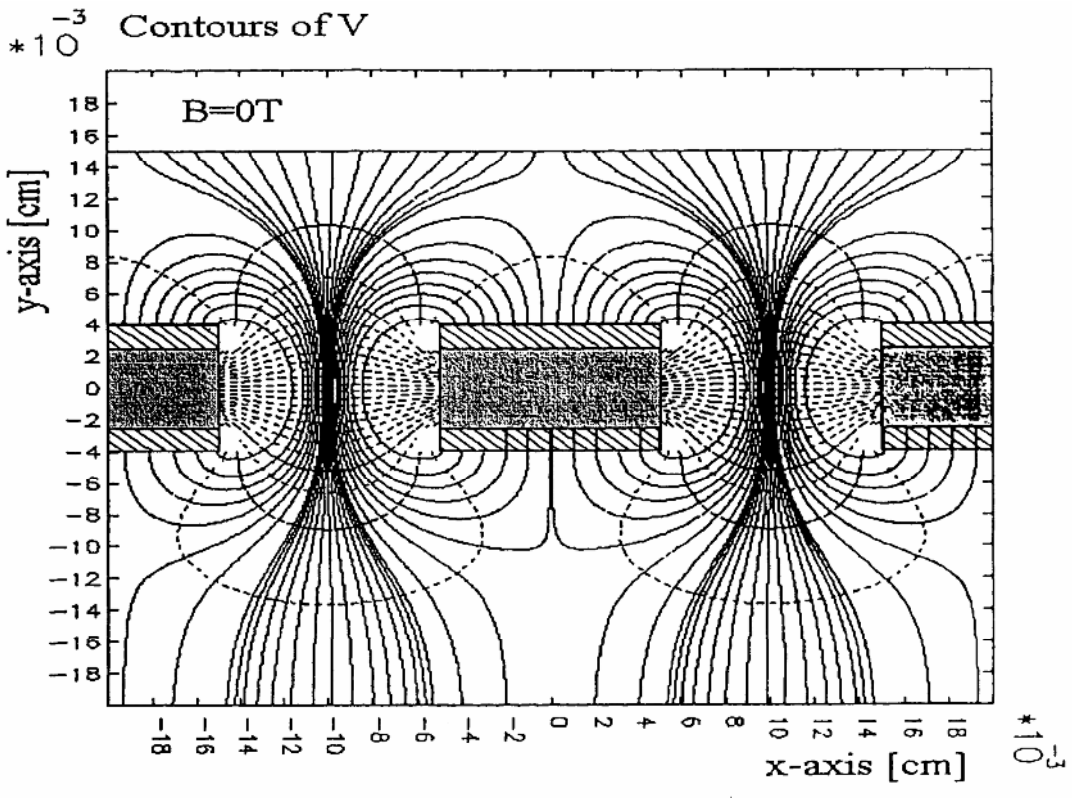

(figs from Hoch, PhD Thesis)

GEM combined with MSGC readout

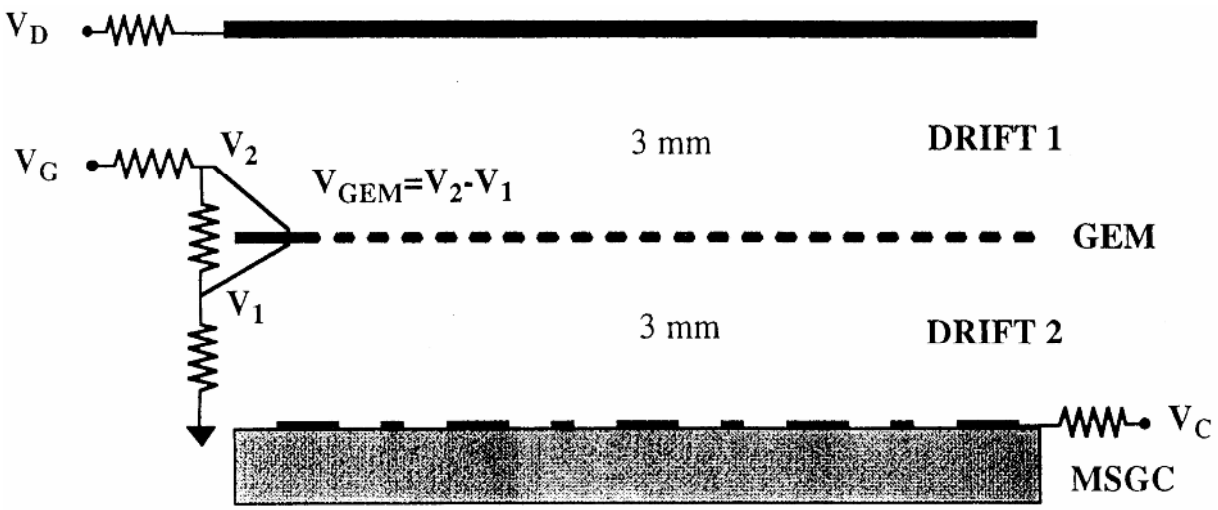

(from Hoch, Kadyk)

Combined gain of GEM + MSGC for various GEM gains

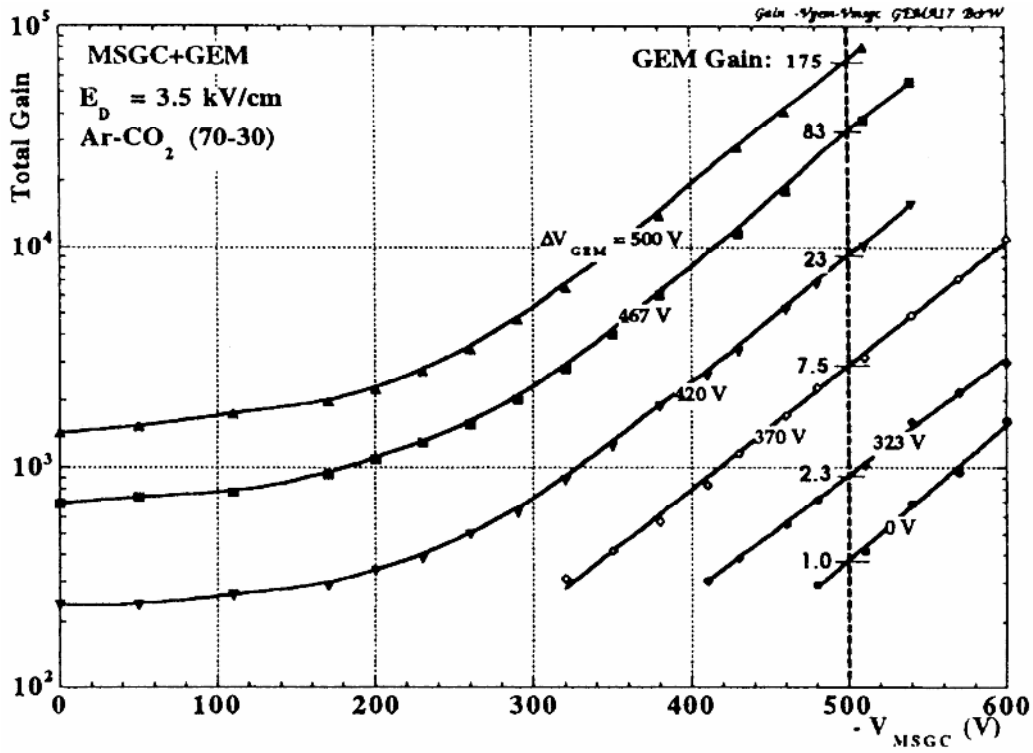

(from Sauli)

Gain of GEM structure alone for various Argon-DME mixtures

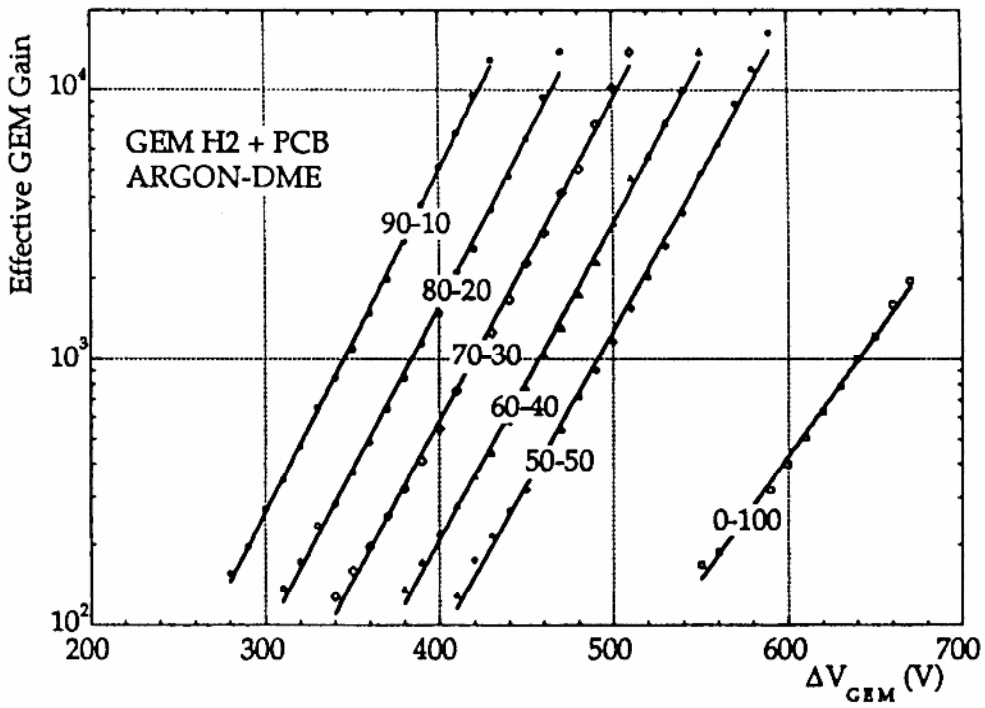

(from Sauli)

GEMs can be cascaded to obtain higher gain

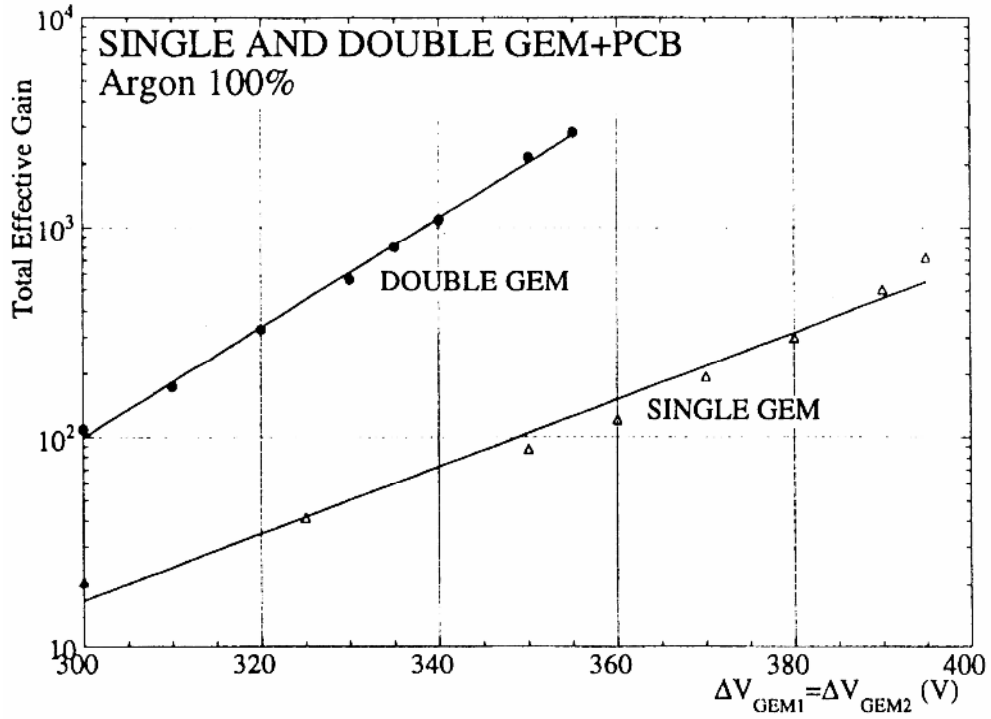

(from Sauli)

GEM fabrication utilizes photolithography and etching

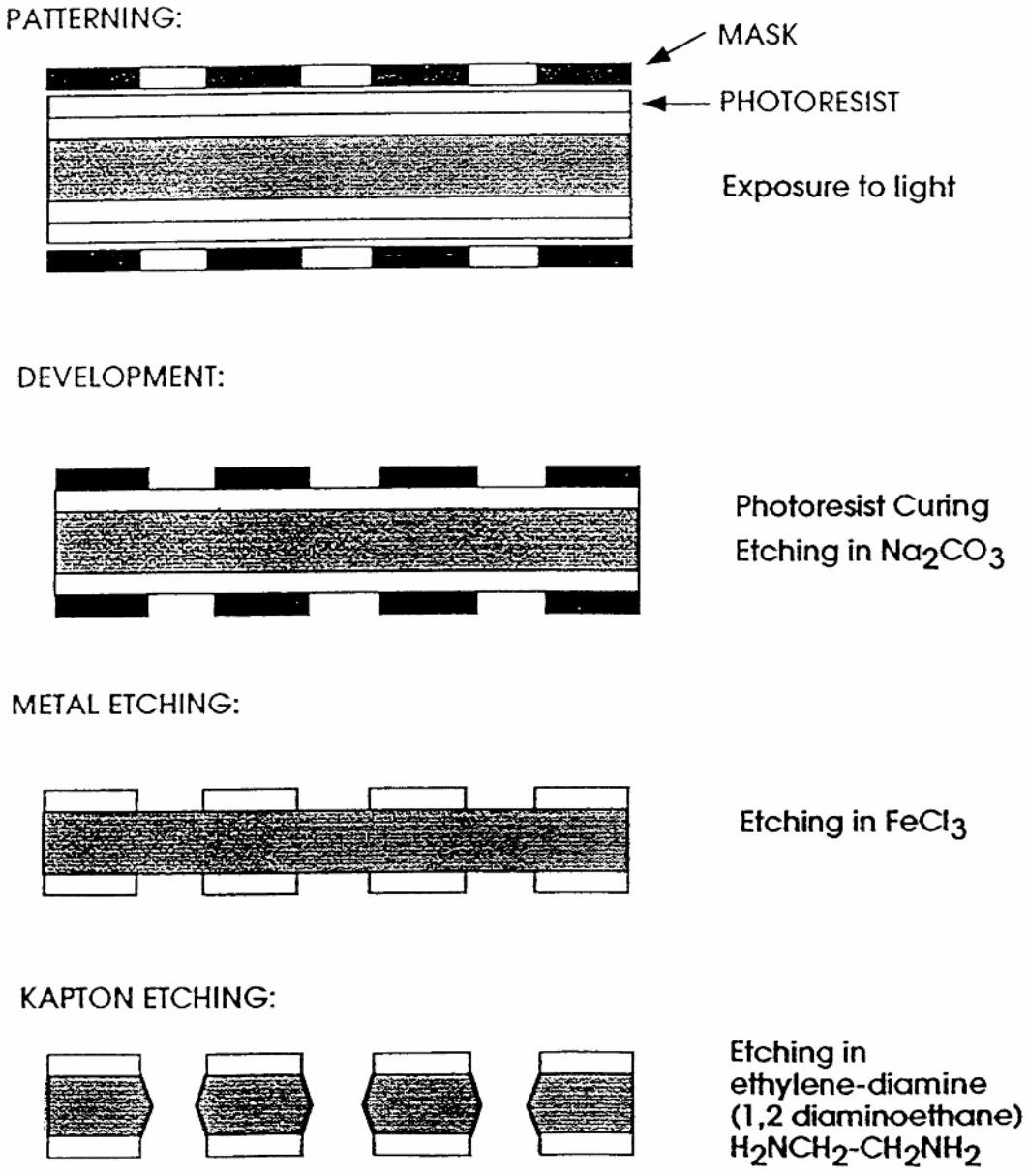

(from Hoch, Kadyk)

Double-sided etching forms a double-conical hole

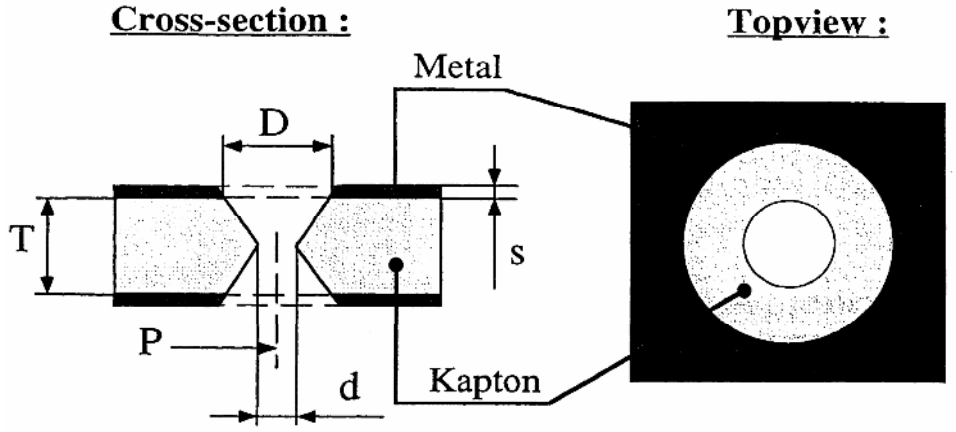

Typical dimensions:

$T =$ 50 μm
$s =$ 5 μm
$D =$ 100 μm
$d =$ 60 μm

Pitch 150 – 200 μm

Field distribution

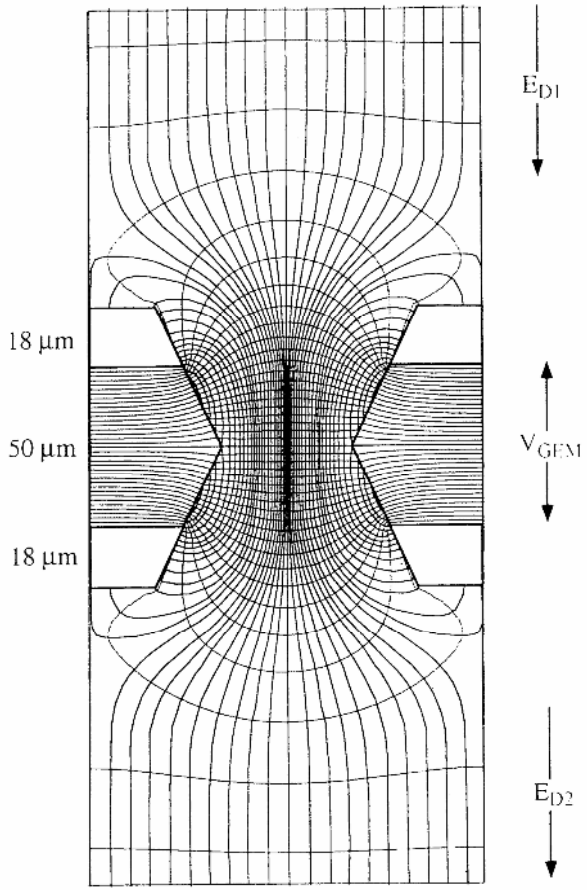

V_{GEM}= 360 V E_{D1}= E_{D2}= 3 kV/cm

(from Hoch, Kadyk, et al.)

Summary

Many types of detectors are used for particle and photon detection.

The “optimum” detector depends on the application.

Frequently, different technologies will provide the required performance.

Combinations of different detector types extend overall detector capabilities.

Practically all modern detectors rely on electronics.